

1 *March 21, 2018*

2  
3 *Submitted to J Hazard Mater*

4  
5  
6 **Deposition and separation of W and Mo from aqueous solutions with**  
7  
8  
9 **simultaneous hydrogen production in stacked bioelectrochemical**  
10  
11 **systems (BESs): Impact of heavy metals W(VI)/Mo(VI) molar ratio,**  
12  
13 **initial pH and electrode material**  
14  
15  
16  
17  
18  
19

20 Liping Huang<sup>1,\*</sup>, Ming Li<sup>1</sup>, Yuzhen Pan<sup>2</sup>, Xie Quan<sup>1</sup>, Jinhui Yang<sup>2</sup>, Gianluca Li Puma<sup>3,\*</sup>

21  
22  
23  
24  
25 1. Key Laboratory of Industrial Ecology and Environmental Engineering, Ministry of  
26 Education (MOE), School of Environmental Science and Technology, Dalian University of  
27 Technology, Dalian 116024, China  
28  
29  
30

31  
32 2. College of Chemistry, Dalian University of Technology, Dalian 116024, China  
33

34  
35 3. Environmental Nanocatalysis & Photoreaction Engineering, Department of Chemical  
36 Engineering, Loughborough University, Loughborough LE11 3TU, United Kingdom  
37  
38  
39  
40  
41  
42  
43  
44  
45  
46

47 **Corresponding authors:**

48 (L. Huang) [lipinghuang@dlut.edu.cn](mailto:lipinghuang@dlut.edu.cn)

49  
50 (G. Li Puma) [g.lipuma@lboro.ac.uk](mailto:g.lipuma@lboro.ac.uk)  
51  
52  
53  
54  
55  
56  
57

58 The authors declare no competing financial interest.  
59  
60  
61

1           **Abstract:** The deposition and separation of W and Mo from aqueous solutions  
2  
3 with simultaneous hydrogen production was investigated in stacked  
4  
5 bioelectrochemical systems (BESs) composed of microbial electrolysis cell (1#)  
6  
7 serially connected with parallel connected microbial fuel cell (2#). The impact of  
8  
9 W/Mo molar ratio (in the range 0.01 mM : 1 mM and vice-versa), initial pH (1.5 to  
10  
11 4.0) and cathode material (stainless steel mesh (SSM), carbon rod (CR) and titanium  
12  
13 sheet (TS)) on the BES performance was systematically investigated. The  
14  
15 concentration of Mo(VI) was more influential than W(VI) in determining the rate of  
16  
17 deposition of both metals and the rate of hydrogen production. Complete metal  
18  
19 recovery was achieved at equimolar W/Mo ratio of 0.05 mM : 0.05 mM. The rates of  
20  
21 metal deposition and hydrogen production increased at acidic pH, with the fastest  
22  
23 rates at pH 1.5. The morphology of the metal deposits and the valence of the Mo were  
24  
25 correlated with W/Mo ratio and pH. CR cathodes (2#) coupled with SSM cathodes  
26  
27 (1#) achieved a significant rate of hydrogen production ( $0.82 \pm 0.04 \text{ m}^3/\text{m}^3/\text{d}$ ) with W  
28  
29 and Mo deposition ( $0.049 \pm 0.003 \text{ mmol/L/h}$  and  $0.140 \pm 0.004 \text{ mmol/L/h}$  (1#);  $0.025$   
30  
31  $\pm 0.001 \text{ mmol/L/h}$  and  $0.090 \pm 0.006 \text{ mmol/L/h}$  (2#)).  
32  
33  
34  
35  
36  
37  
38  
39  
40  
41  
42  
43  
44  
45  
46

47           **Keywords:** Bioelectrochemical system; microbial fuel cell; microbial electrolysis  
48  
49 cells; W and Mo deposition; hydrogen production  
50  
51  
52  
53  
54  
55  
56  
57  
58  
59  
60  
61  
62  
63  
64  
65

## 1 Introduction

Tungsten (W) and molybdenum (Mo) transition metals are valuable alloying resources used in various products such as electrochromic materials, gas sensors and lithium ion batteries, in addition to be contained in a range of materials such as special steels and catalysts for petrochemical industries [1-2]. The 2011 annual global production of W and Mo has been reported as 73000 t and 264000 t respectively, with over 80% of W and nearly 40% of Mo being produced in China [3-4]. The extraction of W and Mo from natural ores is an energy intensive process, requiring approximately 11600 kWh/ton of products [5]. The ore dressing wastewater produced during the extraction process of the metals contains a large amount of W and Mo ranging from 10 mg/L to 1000 mg/L, in addition to their existence in the leaching liquor of the spent industrial products [3,6]. The environmental and economic sustainability of the mining process, therefore, requires the recovery and separation of W and Mo from the leaching liquor and from industrial wastewater.

Conventional processes that have been proposed for the extraction and recovery of W and Mo from mining ores include solvent extraction, ion exchange, membrane separation, chemical precipitation and electrochemical treatment [3,7-9]. However, significant challenges remain, including the reduction of the energy consumption and the treatment cost, the reduction of the sludge produced during the treatment and the requirement of bringing the concentration levels of W(VI) and Mo(VI) in the wastewater effluents below the required environmental standards.

This study addresses novel bioelectrochemical systems (BESs) which may

1 provide an alternative and innovative method for the simultaneous recovery and  
2  
3 separation of W and Mo from industrial and mining aqueous effluents [10]. BES  
4  
5 multifunctional metallurgical processes have been conceived and intensively  
6  
7 investigated, in recent years since they provides cost-effective methods for the  
8  
9 extraction and separation of metals [11-12]. In BESs organic matter is oxidized in the  
10  
11 anodic chamber while dissolved metals may be simultaneously either reduced in the  
12  
13 cathodic chamber or oxidized in the anodic chamber, with the potential of producing  
14  
15 free energy [11-14]. BESs operate with zero or minimal external energy consumption,  
16  
17 generate very little sludge and require minimal reactor maintenance [15-18]. Multiple  
18  
19 metals including V(V), Cr(VI), As(III), Tl (I), Cd(II), Mn(II), Co(II), Ni(II) and Cu(II)  
20  
21 [11-12,16,19-27] have been recovered in single units of either microbial fuel cell  
22  
23 (MFC) or microbial electrolysis cell (MEC). Differently, stacked metallurgical BESs,  
24  
25 configured with MFC units providing in-situ the voltage output to drive the operation  
26  
27 of electrically connected MECs, exhibited more merits than single MFC or MEC units.  
28  
29 Stacked metallurgical BESs have been conceptually explored for the recovering and  
30  
31 separation of multiple metals such as, Cr(VI), Cu(II) and Cd(II), Cu(II) and Co(II),  
32  
33 and Cu(II), Co(II) and Li(I) [28-32]. The concept of using optimized MFC and MEC  
34  
35 stacked BESs for the efficient deposition and separation of W(VI) and Mo(VI) from  
36  
37 mixed aqueous solutions with simultaneous hydrogen production has been  
38  
39 demonstrated in our recent study [10] using an initial pH of 2.0, a W(VI)/Mo(VI)  
40  
41 molar ratio of 1 : 1 and a stainless steel sheet cathode electrode. However, the impact  
42  
43 of the operating parameters require further investigation, in order to optimize the  
44  
45  
46  
47  
48  
49  
50  
51  
52  
53  
54  
55  
56  
57  
58  
59  
60  
61  
62  
63  
64  
65

1 deposition, separation and recovery of W and Mo metals from practical wastes and  
2  
3 wastewaters, with simultaneous hydrogen production.  
4  
5

6 The concentrations of W(VI) and Mo(VI) in the ores and leaching liquor of spent  
7  
8 catalysts are dependent on the characteristics of the mining site or industrial process,  
9  
10 with some cases presenting an excess of Mo(VI) and lower amount of W(VI) or  
11  
12 vice-versa [4-6,9]. The concentrations of W(VI) and Mo(VI) in the ore dressing  
13  
14 wastewater produced during the extraction process, are also closely correlated with  
15  
16 the extraction process used. Thus, significant fluctuations in the concentrations of  
17  
18 W(VI) and Mo(VI) in the wastewater generally occurs [3,5-6], which translates in  
19  
20 variable rates of W and Mo deposition, and thus variable rates of hydrogen production  
21  
22 in the MEC units of the stacked BESs. Similarly, pH plays a significant role on the  
23  
24 nature of the W and Mo ionic forms present in aqueous solution, on the degree of  
25  
26 polymerization of W in electrochemical processes [33], and on the rate of hydrogen  
27  
28 evolution in MECs [34-35]. Furthermore, the cathode material also plays an important  
29  
30 role. A range of cathodes materials including carbon rod, carbon plate, stainless steel  
31  
32 mesh and titanium sheet have been proposed for the recovery of Co(II), Cu(II) and/or  
33  
34 Cd(II) in single MFC or MEC units and even stacked BESs [29-31,36-39]. However,  
35  
36 the performance of only a few of them has been compared under the same operational  
37  
38 conditions [30]. The materials used to recover W and Mo in conventional  
39  
40 electrochemical processes operated under galvanic mode include titanium, platinum,  
41  
42 nickel, copper and gold [2,40-41]. In particular, W and Mo deposits on these materials  
43  
44 also may act as catalysts for the evolution of hydrogen [40-42]. Therefore, the  
45  
46  
47  
48  
49  
50  
51  
52  
53  
54  
55  
56  
57  
58  
59  
60  
61  
62  
63  
64  
65

1 reduction of heavy metals and the reduction of protons to hydrogen may be competing  
2  
3 processes for the cathodic electrons, particularly at low metal concentrations  
4  
5 [37-38,43]. Such occurrence may call for the use of different cathodic material and/or  
6  
7  
8 experimental conditions depending on the desired treatment objectives.  
9

10  
11 In this study, stacked BESs were constructed to investigate the impact of the  
12  
13 W(VI)/Mo(VI) molar ratio (herein reported as W/Mo for brevity), the initial pH and  
14  
15 the cathode electrode material on the rates of W and Mo deposition from aqueous  
16  
17 solutions, and on the simultaneous rates of hydrogen production. The W and Mo  
18  
19 molar ratio was varied in the range of 0.01 : 1 and vice-versa. The initial pH in the  
20  
21 cathodic chamber containing the mixed metals ranged from 1.5 to 4.0, and stainless  
22  
23 steel mesh (SSM), carbon rod (CR) and titanium sheet (TS) were systematically  
24  
25 explored as cathode materials. The BESs system performance was elucidated by  
26  
27 linear sweep voltammetry (LSV), scanning electronic microscopy (SEM), X-ray  
28  
29 photoelectron spectroscopy (XPS) and electrochemical impedance spectroscopy (EIS).  
30  
31 Cathode potential, current and voltage output from the MFC units applied to the  
32  
33 MECs (applied voltage) were employed to assess the rate of W and Mo deposition,  
34  
35 the metals separation factor and the rate of hydrogen production. The concept of  
36  
37 complete metal recovery was also investigated.  
38  
39  
40  
41  
42  
43  
44  
45  
46  
47  
48

## 49 **2 Materials and Methods**

### 50 *2.1 BESs assembly*

51  
52 Stacked BESs were designed with one MFC (1#) serially connected with three  
53  
54 parallel MFCs (2#) (Fig. S1) as a result of previous optimization of the modules with  
55  
56  
57  
58  
59  
60  
61  
62  
63  
64  
65

1 multiple units [10]. Each reactor unit was made of two-chambers (14 ml operating  
2  
3 volume) separated by a cation exchange membrane (CMI-7000 Membranes  
4  
5 International, Glen Rock, NJ). Porous graphite felts ( $1.0 \times 1.0 \times 1.0$  cm, San Ye Co.,  
6  
7 Beijing, China) were used as anodes [44], whereas SSS ( $2.0 \times 2.0$  cm, Qing Yuan Co.,  
8  
9 China) were used as the cathodes of both the 1# and the 2# units. A glass tube with an  
10  
11 inner diameter of 8 mm was glued to the top of the 1# unit to create a total headspace  
12  
13 of 12 mL for hydrogen collection [10,44]. A reference electrode (Ag/AgCl, 195 mV vs.  
14  
15 SHE) was installed in the cathodic chamber to measure the electrode potential, with  
16  
17 all potentials reported vs. SHE. The reactors were wrapped with aluminum foil to  
18  
19 ensure darkness, to avoid the algae growth on the anodes and possible side reactions  
20  
21 on the cathodes. The properties of the 2# units have been reported as average values  
22  
23 for the sake of clarity, since the differences among the three units connected in  
24  
25 parallel were insignificant.  
26  
27  
28  
29  
30  
31  
32  
33  
34

## 35 36 2.2 Inoculation and operation

37  
38 Anodic inoculation was exactly the same as previously described [28-30]. Mixed  
39  
40 W(VI) and Mo(VI) aqueous solutions were prepared using  $\text{Na}_2\text{WO}_4 \cdot 2\text{H}_2\text{O}$  and  
41  
42  $\text{Na}_2\text{MoO}_4 \cdot 2\text{H}_2\text{O}$  (Kaida Chemical Co. Ltd., Tianjin, China). The W and Mo molar  
43  
44 ratio (mM : mM) in the cathodic chamber was varied as 1 : 1, 0.1 : 1, 0.05 : 1, 0.01 :  
45  
46 1, 1 : 0.1, 1 : 0.05, and 1 : 0.01, and the initial pH was 1.5, 2.0, 2.5, 3.0, 3.5 and 4.0.  
47  
48 Also experiments were conducted at equimolar concentrations of 0.1 : 0.1 and 0.05 :  
49  
50 0.05. Solution conductivity was invariably regulated to the maximal 6.60 mS/cm  
51  
52 associated with the most acidic pH of 1.5, to exclude the effect of solution  
53  
54  
55  
56  
57  
58  
59  
60  
61  
62  
63  
64  
65

1 conductivity on system performance [45]. SSM, CR (Chijiu Duratight Carbon Co.,  
2  
3 Qingdao, China) or TS (Qingyuan Co., China) cathodes (1#) were coupled with  
4  
5  
6 SSM or CR cathodes (2#) with equal geometric areas ( $2.0 \times 2.0$  cm). The stacked  
7  
8  
9 BESs were operated in fed-batch mode at room temperature ( $25 \pm 3$  °C). Three  
10  
11  
12 duplicate BESs were used in all experiments.

13  
14 Control experiments with single W(VI) or Mo(VI) metal in solution were  
15  
16 performed to reflect the impact of the binary-component on the system performance.  
17  
18 Control experiments under open circuit conditions (OCCs) reflected the effect of  
19  
20 current on W and Mo deposition. Other control experiments using the 1# or the 2#  
21  
22  
23 units only were performed to illustrate the roles played by each unit on system  
24  
25  
26  
27 performance.

### 28 29 30 31 *2.3 Measurements and analyses*

32  
33 The W(VI) and Mo(VI) concentrations in the catholyte were measured using  
34  
35 standard methods [46]. The electrical data were monitored with an automatic data  
36  
37 acquisition system (PISO-813, Hongge Co.,Taiwan). The electrical current was  
38  
39 calculated from the voltage read across a small external resistance ( $10 \Omega$ ). The  
40  
41  
42 hydrogen in the headspace of the cathodic chambers was sampled and analyzed as  
43  
44  
45 previously described [10,37-38,44].

46  
47  
48 The rates of W ( $R_W$ , mmol/L/h) and Mo ( $R_{Mo}$ , mmol/L/h) deposition on the  
49  
50  
51 cathodes was calculated from Eqs. S1 – 2, whereas the power density was normalized  
52  
53 to the projected surface area of the separator [10]. The rate of hydrogen production  
54  
55  
56 and the separation factor  $\varepsilon$  were calculated from Eqs. S3 and S4, respectively [10,36].  
57  
58  
59  
60  
61  
62  
63  
64  
65



1 LSVs were conducted using a potentiostat (CHI 770c, Chenhua, Shanghai) at a scan  
2  
3 rate of 1.0 mV/s. The inner resistance of the BES units at different initial pH and  
4  
5  
6 W/Mo molar ratios was quantified by EIS (Bio-Logic VMP3) as previously described  
7  
8  
9 [10,39,43,47]. The morphologies and valences of the products on the cathode were  
10  
11 observed by SEM (Hitachi S-4800) and determined by XPS (Kratos AXIS Ultra  
12  
13 DLD). One-way ANOVA in SPSS 19.0 was used to analyze the differences among the  
14  
15 data, and all of the data indicated significance levels of  $p < 0.05$ .  
16  
17  
18  
19

### 20 **3 Results and discussion**

#### 21 *3.1 The impact of W/ Mo molar ratio*

22  
23  
24  
25 At a fixed Mo concentration of 1.0 mM, higher W concentrations favored the  
26  
27 deposition of W (Fig. 1A) and negligibly affected the deposition of Mo (Fig. 1B) in  
28  
29 both the 1# and the 2# units. The rate of deposition of W was  $0.079 \pm 0.003$  mmol/L/h  
30  
31 (1#) and  $0.050 \pm 0.001$  mmol/L/h (2#) (Fig. 1A), while for Mo it was  $0.193 \pm 0.002$   
32  
33 mmol/L/h (1#) and  $0.138 \pm 0.001$  mmol/L/h (2#) (Fig. 1B), at the higher  
34  
35 concentration of W investigated (1.0 mM). Greater amounts of W and Mo were  
36  
37 invariably deposited in the 1# unit, rather than in the 2# units (Fig. 1A and B), which  
38  
39 was ascribed to the voltage output from the 2# units and applied to the 1# unit (Fig.  
40  
41 1C) for the consequent higher currents (Fig. 1D) and more negative cathode potentials  
42  
43 (Fig. 1E) in the 1# unit. Higher current and more negative potentials favor the rate of  
44  
45 deposition of oxidative metals on the cathodes of BESs [11-12]. The observed  
46  
47 polarization curves and electrode potentials as a function of the current (Fig. S2)  
48  
49 further demonstrated the significance and impact of the W concentration on the BESs  
50  
51  
52  
53  
54  
55  
56  
57  
58  
59  
60  
61  
62  
63  
64  
65

1 performance. The similar values of applied voltages, in the range 0.10 – 0.11 V (Fig.  
2  
3 1C), led to the simultaneous evolution of hydrogen at variable rates (0.34 – 0.41  
4  
5  $\text{m}^3/\text{m}^3 \text{ d}$ ) in the 1# unit, during the deposition of the metals (Fig. 1F). This result also  
6  
7 reflected an insignificant effect of W concentrations on the rate of hydrogen  
8  
9 production in the 1# unit.  
10  
11  
12

### 13 Here Fig. 1

14  
15  
16 At a fixed W concentration of 1.0 mM, a decrease in Mo concentration decreased  
17  
18 the rate of deposition of W (Fig. 2A) and Mo (Fig. 2B) in both the 1# and the 2# units  
19  
20 with varying degrees. This resulted in high values of the separation factors equal to  
21  
22 717  $\pm$  4 (1#) and 200  $\pm$  8 (2#), at a W/Mo molar ratio of 1 : 0.1 (Table 1), which were  
23  
24 significantly higher than the values (80 to 105) reported in conventional solvent  
25  
26 extraction processes [8]. Lower Mo concentrations led to decreased currents (Fig. 2C)  
27  
28 and less negative cathode potentials (Fig. 2D) in the 1# unit. It also significantly  
29  
30 decreased the applied voltages (Fig. 2E), consistent with the polarization curves and  
31  
32 the cathodic potentials as a function of current (Fig. S3), all of which explained the  
33  
34 decreased rate of hydrogen production observed (Fig. 2F).  
35  
36  
37  
38  
39  
40  
41  
42  
43

44 Collectively, the results in Fig. 1 and Fig. 2 show that Mo(VI) was more  
45  
46 influential than W(VI) in determining an increase in the rate of deposition of both  
47  
48 metals and in the rate of hydrogen production. The influential role of Mo(VI) for  
49  
50 either W(VI) recovery or as catalysts for hydrogen evolution in conventional  
51  
52 chemical/electrochemical processes has been also shown in other studies [2,7-8,41,48].  
53  
54  
55  
56  
57

58 Binary mixtures of W(VI) and Mo(VI) reportedly forms diverse molybdotungstates  
59  
60  
61

1 species, which favor the further deposition of W(VI), however, the deposition of W is  
2  
3 inhibited in the absence of Mo(VI) in conventional chemical/electrochemical  
4  
5 processes [7,49]. Thus, at high W/Mo molar ratios, the rates of deposition of the  
6  
7 metals and hydrogen production were diminished in the stacked BESs.  
8  
9

10  
11  
12 **Here Fig. 2**

13  
14 **Here Table 1**

15  
16  
17 The W/Mo molar ratio also influenced the morphology of the metals deposited  
18  
19 over the stacked BESs cathodes. Smaller and more homogeneous particles were  
20  
21 observed on the cathodes of both the 1# (Fig. S4A) and the 2# (Fig. S4B) units at a  
22  
23 W/Mo molar ratio of 1 : 0.01, in comparison to those at a W/Mo ratio of 1 : 1 (Fig.  
24  
25 S4C and D). Conversely, a W/Mo molar ratio of 0.01 : 1 led to the presence of  
26  
27 irregular deposits in the 1# unit (Fig. S4E) complemented by dense layer deposits in  
28  
29 the 2# units (Fig. S4F).  
30  
31  
32  
33  
34  
35

36  
37 The XPS spectra for the W4f or Mo3d core electronic transitions exhibited the  
38  
39 characteristic 4f<sub>7/2</sub> and 4f<sub>5/2</sub> or 3d<sub>5/2</sub> and 3d<sub>3/2</sub> doublet of peaks at 35.8 and 37.9 eV  
40  
41 assigned to W(VI) in WO<sub>3</sub> [50], whereas the peaks at 232.9 and 236.0, 231.4 and  
42  
43 234.5, and 230.0 and 233.1 eV corresponded to Mo3d<sub>5/2</sub> and Mo3d<sub>3/2</sub> in MoO<sub>3</sub>,  
44  
45 Mo<sub>2</sub>O<sub>5</sub> and MoO<sub>2</sub>, respectively (Table S1) [42]. Similar peaks at 35.9 and 38.1 eV  
46  
47 were observed in both the 1# (Fig. 3A and E) and the 2# (Fig. 3C and G) units  
48  
49 regardless of the W/Mo molar ratio (i.e., high (1 : 0.01) (Fig. 3A and C) or low (0.01 :  
50  
51 1) (Fig. 3E and G)). The catholyte at the end of each fed-batch cycle operation  
52  
53 instantly changed in color in the absence of N<sub>2</sub> protection, consistent with the report  
54  
55  
56  
57  
58  
59  
60  
61  
62  
63  
64  
65

1 that W(V) as a reduced product is highly unstable and easily oxidized to W(VI) due to  
2  
3 the sampling procedures [2]. Thus, these similar peaks (Fig. 3A, 3C, 3E and 3G)  
4  
5 could presumably be the result from the re-oxidation of the W reduced products. In  
6  
7 contrast, the valence of the Mo deposits was strongly correlated with the W/Mo molar  
8  
9 ratio and varied among the different units (Fig. 3B, D, F and H). Stronger Mo(V) and  
10  
11 Mo(IV) signals were observed at a low W/Mo molar ratio of 0.01 : 1 in the 1# unit  
12  
13 (Fig. 3F) rather than in the 2# units (Fig. 3H and Table S1), while much weaker  
14  
15 signals were observed at a W/Mo molar ratio of 1 : 0.01 in the 1# unit (Fig. 3B and  
16  
17 Table S1). This result demonstrates that Mo(VI) was more easily reduced to Mo(V)  
18  
19 rather than Mo(IV).

### Here Fig. 3

20  
21  
22  
23  
24  
25  
26  
27  
28  
29 The variation of the cathode resistances at different W/Mo molar ratios was  
30  
31 determined by EIS (Fig. 4) through the fitting of the observed spectra to equivalent  
32  
33 electrical circuits (Fig. S5 and Table S2). The ohmic resistance ( $R_o$ ) at low W/Mo  
34  
35 ratios of 0.05 : 1 and 0.01 : 1 was equivalent to that at equimolar W/Mo ratio of 1 : 1,  
36  
37 but the polarization resistance ( $R_p$ ) was higher and the diffusional resistance ( $R_d$ ) was  
38  
39 lower (Fig. 4A and Table S2). Therefore, the deposition of Mo increased the activation  
40  
41 loss and decreased the diffusional loss. High W/Mo ratios instead, invariably  
42  
43 increased the resistances  $R_o$ ,  $R_p$  and  $R_d$  (Fig. 4B and Table S2), consistent with the  
44  
45 polarization curves and cathode potentials as a function of current (Fig. S3), implying  
46  
47 that the W deposits had a stronger effect than Mo on the resistances. In the control  
48  
49 experiments performed with either W(VI) or Mo(VI) in solution, the resistances  $R_o$ ,  
50  
51  $R_p$  and  $R_d$  were appreciably higher than those observed with the binary metals (Fig.

1 4C and Table S2).

2  
3 **Here Fig. 4**

4  
5  
6 *3.2 Effect of initial pH*

7  
8  
9 The initial pH of the catholyte was varied in the range from 1.5 to 4.0. At acidic  
10 pH of 1.5 and 2.0 the highest rates of W and Mo deposition were observed, equaling  
11  
12  $0.0785 \pm 0.003 - 0.0808 \pm 0.004$  mmol/L/h (W) and  $0.190 \pm 0.004 - 0.193 \pm 0.002$   
13  
14 mmol/L/h (Mo) in the 1# unit, and  $0.0501 \pm 0.001 - 0.0548 \pm 0.001$  mmol/L/h (W)  
15  
16 and  $0.138 \pm 0.001 - 0.144 \pm 0.005$  mmol/L/h (Mo) in the 2# units (Fig. 5A and B).  
17  
18 Higher amounts of metals deposited in the 1# than in the 2# units, were generally  
19  
20 accompanied by higher separation factors in the former (Table 1), consistent with the  
21  
22 higher currents (Fig. 5C) and the more negative cathode potentials (Fig. 5D) observed  
23  
24 in the 1# unit, both of which generally favor the reduction of oxidative substrates  
25  
26 [11,51]. A decreasing trend of the rate of metal deposition was observed at an initial  
27  
28 pH higher than 2.0.  
29  
30  
31  
32  
33  
34  
35  
36  
37  
38

39 Smaller polarization loss (Fig. S6), higher applied voltage (Fig. 5E) and an  
40  
41 appreciable higher rate of hydrogen production (Fig. 5F) were observed at more  
42  
43 acidic initial pH in the 1# unit, consistent with the decrease of the pH in the effluents  
44  
45 from  $5.93 \pm 0.08$  at an initial pH of 4.0 to  $2.27 \pm 0.06$  at pH 1.5. Other studies,  
46  
47 performed with MECs in the absence of W or/and Mo also reported faster rates of  
48  
49 hydrogen production at more acidic pH [34-35]. Considering the similar rates of W  
50  
51 and Mo depositions at pH 1.5 and 2.0 (Fig. 5A and B), the significantly higher  
52  
53 hydrogen production at pH 1.5 implied that hydrogen evolution outcompeted the  
54  
55  
56  
57  
58  
59  
60  
61  
62

1 deposition of the metals for the available cathodic electrons, alike the electron  
2  
3 competition between reductive dechlorination and denitrification [52].  
4  
5

6 An experiment with pH controlled at 1.5 during the entire operational period was  
7  
8 purposely investigated to determine its effect on the metal deposition. An appreciable  
9  
10 higher rate of hydrogen production of  $2.14 \pm 0.07 \text{ m}^3/\text{m}^3/\text{d}$ , and enhanced W and Mo  
11  
12 deposition rates (W:  $0.0965 \pm 0.005 \text{ mmol/L/h}$ ; Mo:  $0.227 \pm 0.005 \text{ mmol/L/h}$ ) in the  
13  
14 1# unit were observed, compared to the results obtained without pH control ( $1.21 \pm$   
15  
16  $0.03 \text{ m}^3/\text{m}^3/\text{d}$ ,  $0.081 \pm 0.004 \text{ mmol/L/h}$  (W) and  $0.190 \pm 0.004 \text{ mmol/L/h}$  (Mo)). In  
17  
18 concert, the results observed supported a significant dependence of the rate of W and  
19  
20 Mo deposition with simultaneous hydrogen production on the pH in the catholyte.  
21  
22  
23  
24  
25  
26  
27

### 28 Here Fig. 5

29  
30 The morphology of the W and Mo deposits was significantly influenced by the  
31  
32 initial pH in the catholyte. Wider cracks and larger areas surrounded by the cracks in  
33  
34 both the 1# and the 2# units (Fig. S7A and B) were observed at pH 1.5, in comparison  
35  
36 to the results at pH 2.0 and 4.0, consistent with the morphology of Mn, Mo and W  
37  
38 co-deposits in conventional electrochemical processes [33]. Larger W and Mo grain  
39  
40 sizes were consistently observed in the 1# (Fig. S7A, C and E) than in the 2# units  
41  
42 (Fig. S7B, D and F), and the grain size was inversely correlated with the increase in  
43  
44 the initial pH in the same units. The higher currents observed in the 1# than in the 2#  
45  
46 units at the same pH (Fig. 5C) resulted in wider cracks and smaller grains, consistent  
47  
48 with the tungsten morphology influenced by current in conventional electrochemical  
49  
50 processes [53].  
51  
52  
53  
54  
55  
56  
57  
58  
59  
60  
61  
62  
63  
64  
65

1 The XPS binding energies (Fig. 6) for Mo and W deposits as well as the  
2  
3 corresponding area percent (Table S1) showed that at an initial pH 1.5 appreciable  
4  
5 higher Mo(IV) products were achieved in the 1# unit (48%, Fig. 6B and Table S2)  
6  
7 than in the 2 units (26%, Fig. 6F and Table S2), both of which were higher than the  
8  
9 results at an initial pH of 4.0 (13% in 1#, Fig. 6D and 8% in 2#, Fig. 6H and Table S2).  
10  
11 These results clearly demonstrate the dependency of the valences of the Mo deposits  
12  
13 on the initial pH. Similarly, the peaks associated with W deposits in the 1# unit at pH  
14  
15 1.5 (Fig. 6A) were apparently higher than either in the 2# units at the same pH (Fig.  
16  
17 6E) or in the same 1# unit but at pH 4.0 (Fig. 6C). The lowest peaks were observed in  
18  
19 the 2# units at pH 4.0 (Fig. 6G). Collectively, these results demonstrated a significant  
20  
21 dependency of the rate of W and Mo deposition, and even the dependence of the  
22  
23 valence of the Mo deposits, on the initial pH of the catholyte, and on the units of the  
24  
25 stacked BESs.  
26  
27  
28  
29  
30  
31  
32  
33  
34

### 35 Here Fig. 6

36  
37  
38  
39 EIS spectra were used to identify the components of the internal resistances as a  
40  
41 function of the initial pH.  $R_d$ ,  $R_p$  and  $R_o$  in concert exhibited increase trends with an  
42  
43 increase in the initial pH, from 456  $\Omega$ , 10.1  $\Omega$  and 6.9  $\Omega$  at a pH of 1.5, to 11987  $\Omega$ ,  
44  
45 121.1  $\Omega$  and 17.8  $\Omega$  at pH 4.0 (Fig. S8 and Table S2). These results clearly illustrated  
46  
47 the favorable effect of acidic pH on decreasing the internal resistances of the stacked  
48  
49 BESs, consistent with the results shown in Fig. 5.  
50  
51  
52

### 53 3.3 Effect of electrode material

54  
55  
56  
57  
58 The use of inexpensive SSS cathodes in both the 1# and the 2# units achieved the  
59  
60  
61

1 highest rate of W (Fig. 7A) and Mo deposition (Fig. 7B) with lower rates of hydrogen  
2  
3 production (Fig. 7F) and more polarization loss (Fig. S9A and B), in comparison to  
4  
5 the other electrodes combinations tested (Fig. 7A, B and F, Fig. S9). SSS cathodes (1#)  
6  
7 coupled with the CR cathodes (2#) exhibited similar more negative cathode potentials  
8  
9 and higher currents as the configuration using TS (1# unit) and CR (2#) cathodes (Fig.  
10  
11 7C and D), resulting in higher applied voltages (Fig. 7E) and the subsequent  
12  
13 significant rate of hydrogen production of  $0.82 \pm 0.04 \text{ m}^3/\text{m}^3/\text{d}$  (Fig. 7F) with W and  
14  
15 Mo deposition (W:  $0.049 \pm 0.003 \text{ mmol/L/h}$  (1#),  $0.025 \pm 0.001 \text{ mmol/L/h}$  (2#); Mo:  
16  
17  $0.140 \pm 0.004 \text{ mmol/L/h}$  (1#),  $0.090 \pm 0.006 \text{ mmol/L/h}$  (2#)) (Fig. 7A and B).  
18  
19 Hydrogen evolution is well known to increase the pH in solution [34], which in  
20  
21 consequence penalizes the deposition of W and Mo [10], explaining reduced rates of  
22  
23 W and Mo deposition at much more negative cathode potentials and higher currents  
24  
25 (Fig. 7A – D). The results collectively show that SSS (1#) and CR (2 #) represent  
26  
27 well-matched electrodes for efficient W and Mo deposition in the stacked BESs.  
28  
29  
30  
31  
32  
33  
34  
35  
36  
37  
38

39 **Here Fig. 7**

### 40 *3.4 Complete metal recovery*

41  
42 The results reported have shown that the W(VI)/Mo(VI) molar ratio significantly  
43  
44 affected the rate of metals deposition, as well as, the rate of hydrogen production in  
45  
46 the stacked BESs. W(VI)/Mo(VI) molar ratios smaller or equal to 1 : 1 favoured the  
47  
48 deposition of more W and Mo in the 1# than the 2# units with a negligible effect on  
49  
50 the rate of hydrogen production (Fig. 1). In contrast, W(VI)/Mo(VI) molar ratios  
51  
52 larger than 1 : 1 resulted in similar rates of deposition of both metals in both the 1#  
53  
54  
55  
56  
57  
58  
59  
60  
61  
62



1 and the 2# units, and more than halved the rate of hydrogen production (Fig. 2).  
2  
3 Further experiments with equimolar W(VI)/Mo(VI) molar ratios and lower initial  
4 metals concentrations (1 : 1, 0.1 : 0.1 and 0.05 : 0.05) were performed at an initial pH  
5  
6 of 2.0 with cathodes of SSS (1#) and CR (2#) to clarify the role of equimolar heavy  
7  
8 metals concentration on system performance. The rates of W (Fig. 8A) and Mo (Fig.  
9  
10 8B) deposition decreased when reducing the concentrations of the metals from 1 : 1 to  
11  
12 0.05 : 0.05. At the lower metals concentrations of 0.05 : 0.05, complete heavy metals  
13  
14 deposition was achieved in the 1# unit and almost complete deposition ( $94.3 \pm 2.2\%$   
15  
16 (W) and  $98.4 \pm 0.8\%$  (Mo)) occurred in the 2# units. Simultaneously, lower separation  
17  
18 factors (Table 1), smaller currents (Fig. 8C), more positive cathode potentials (Fig.  
19  
20 8D), lower applied voltages (Fig. 8E) and smaller rates of hydrogen production (Fig.  
21  
22 8F) were observed in comparison to the 1 : 1 case. These results demonstrate the  
23  
24 feasibility of these stacked BESs for either complete deposition of W and Mo at this  
25  
26 lower equivalent W and Mo concentrations, or higher rates of hydrogen production at  
27  
28 higher equivalent W and Mo concentrations.  
29  
30  
31  
32  
33  
34  
35  
36  
37  
38  
39  
40  
41

### 42 Here Fig. 8

43  
44 The deposition of binary mixtures of W(VI) and Mo(VI) in stacked BESs have  
45  
46 shown synergistic effects on the recovery of the metals and the simultaneous  
47  
48 production of hydrogen [10]. However, the optimization of such BESs required  
49  
50 further analysis to account for the impact of fluctuations in the concentration of heavy  
51  
52 metals and pH in the wastewater [4-6]. Furthermore, the electrode materials exert a  
53  
54 significant impact on the rates of other metals deposition and hydrogen production in  
55  
56  
57  
58  
59  
60  
61  
62  
63  
64  
65

1 BESs [35,37-37,54]. The elucidation of such effects is required for further  
2  
3 optimization of BESs, which could ultimately lead to industrial application.  
4  
5

6 The present study has illustrated the dependency of rates of W and Mo  
7  
8 deposition, as well as, hydrogen production on the W/Mo molar ratio, initial pH and  
9  
10 electrode material. Mo(VI) was more influential than W(VI) in determining an  
11  
12 increase in the rates of deposition of both metals and hydrogen production. The merit  
13  
14 of completely depositing W and Mo at an initial equimolar W/Mo ratio of 0.05 : 0.05  
15  
16 gives an advantage of this technology over conventional methods such as ion  
17  
18 exchange, chemical precipitation or adsorption [5,9], particularly with low-strength W  
19  
20 and Mo wastewaters from either the mining industry processes or wastewater  
21  
22 effluents. Such lower concentrations of metals in high strength wastewater could be  
23  
24 achieved with the partial recirculation of the effluent back to the influent [55-56] to  
25  
26 dilute the feed stream to the stacked BESs to optimal values, achieving enhanced  
27  
28 metal deposition and even complete separation of W and Mo (Fig. 1,2 and 8, and  
29  
30 Table 1). Practical implementation will also depend on the long-term operation of this  
31  
32 system, as well as, the process economics of BESs relative to conventional treatment  
33  
34 processes [54]. Although the present economic values of W and Mo deposits are  
35  
36 relatively low, the added complexity in the stacked BESs will be paid off with  
37  
38 increasing the demand on sustainability and elevated product values due to the  
39  
40 depletion of W and Mo resources. The simultaneous production of hydrogen  
41  
42 by-product in the MEC units of the stacked BESs further offsets the cost of this  
43  
44 technology, although further pilot and full-scale investigations are necessary to  
45  
46  
47  
48  
49  
50  
51  
52  
53  
54  
55  
56  
57  
58  
59  
60  
61  
62  
63  
64  
65

1 evaluate the long-term operation and stability of the system over feeds with  
2  
3 fluctuating physico/chemical properties.  
4  
5

#### 6 **4 Conclusions**

7  
8  
9 Stacked BESs composed of MEC (1#) serially connected with parallel connected  
10  
11 MFC (2#) have been shown to be effective in W and Mo deposition and separation  
12  
13 with simultaneous hydrogen production. It revealed a dramatic effect of the W/Mo  
14  
15 molar ratio, initial pH, and cathode material on the rates observed. The concentration  
16  
17 of Mo(VI) was more influential than W(VI) in determining the rate of deposition of  
18  
19 both metals and the rate of hydrogen production. Complete metal recovery was  
20  
21 achieved at equimolar W/Mo ratio of 0.05 mM : 0.05 mM. Acidic pH favored both the  
22  
23 deposition of the metals and the rate of hydrogen production. The BESs comprising  
24  
25 CR cathodes (2#) coupled with SSS cathodes (1#) achieved optimal performance. The  
26  
27 BESs studied here may provide an alternative and innovative method for the recovery  
28  
29 and separation of W and Mo from industrial and mining aqueous effluents with  
30  
31 simultaneous hydrogen production.  
32  
33  
34  
35  
36  
37  
38  
39  
40  
41  
42  
43  
44

#### 45 **Acknowledgments**

46  
47 The authors are gratefully acknowledge financial support from the National  
48  
49 Natural Science Foundation of China (Nos. 51578104 and 21777017), and the  
50  
51 Programme of Introducing Talents of Discipline to Universities (B13012).  
52  
53  
54

#### 55 **References**

56  
57 [1] D. Merki, X. Hu, Recent developments of molybdenum and tungsten sulfides as  
58  
59 hydrogen evolution catalysts, *Energy Environ. Sci.* 4 (2011) 3878-3888,  
60  
61 <http://dx.doi.org/10.1039/C1EE01970H>.  
62

- 1 [2] S. Sun, T. Bairachna, E.J. Podlaha, Induced codeposition behavior of  
2 electrodeposited NiMoW alloys, *J. Electrochem. Soc.* 160 (2013) D434-D440,  
3 <http://dx.doi.org/10.1149/2.014310jes>.
- 4 [3] T.A. Lasheen, M.E. El-Ahmady, H.B. Hassib, A.S. Helal, Molybdenum metallurgy  
5 review: Hydrometallurgical routes to recovery of molybdenum from ores and  
6 mineral raw materials, *Miner. Process. Extr. Metall. Rev.* 36 (2015)145-173,  
7 <http://dx.doi.org/10.1080/08827508.2013.868347>.
- 8 [4] T. Ogi, T. Makino, K. Okuyama, W.J. Stark, F. Iskandar, Selective biosorption and  
9 recovery of tungsten from an urban mine and feasibility evaluation, *Ind. Eng. Chem.*  
10 *Res.* 55 (2016) 2903-2910, <http://dx.doi.org/10.1021/acs.iecr.5b04843>.
- 11 [5] Z. Zhao, C. Cao, X. Chen, G. Huo, Separation of macro amounts of tungsten and  
12 molybdenum by selective precipitation, *Hydrometallurgy* 108 (2011) 229-232,  
13 <https://doi.org/10.1016/j.hydromet.2011.04.006>.
- 14 [6] R.R. Srivastava, N.K. Mittal, B. Padh, B. Ramachandra Reddy, Removal of  
15 tungsten and other impurities from spent HDS catalyst leach liquor by an  
16 adsorption route, *Hydrometallurgy* 127-128 (2012) 77-83,  
17 <https://doi.org/10.1016/j.hydromet.2012.07.004>.
- 18 [7] L. Kondrachova, P.H. Benjamin, G. Vijayaraghavan, R.D. Williams, K.J.  
19 Stevenson, Cathodic electrodeposition of mixed molybdenum tungsten oxides from  
20 peroxo-polymolybdotungstate solutions, *Langmuir* 22 (2006) 10490-10498,  
21 <https://doi.org/10.1021/la061299n>.
- 22 [8] W. Guan, G. Zhang, C. Gao, Solvent extraction separation of molybdenum and  
23 tungsten from ammonium solution by H<sub>2</sub>O<sub>2</sub>-complexation, *Hydrometallurgy*  
24 127-128 (2012) 84-90, <https://doi.org/10.1016/j.hydromet.2012.07.008>.
- 25 [9] G. Huo, C. Peng, Q. Song, X. Lu, Tungsten removal from molybdate solutions  
26 using ion exchange, *Hydrometallurgy* 147-148 (2014) 217-222,  
27 <https://doi.org/10.1016/j.hydromet.2014.05.015>.
- 28 [10] L. Huang, M. Li, Y. Pan, Y. Shi, X. Quan, G. Li Puma, Efficient W and Mo  
29 deposition and separation with simultaneous hydrogen production in stacked  
30 bioelectrochemical systems, *Chem. Eng. J.* 327 (2017) 584-596,  
31 <http://dx.doi.org/10.1016/j.cej.2017.06.149>.
- 32 [11] H. Wang, Z.J. Ren, Bioelectrochemical metal recovery from wastewater: a review,  
33 *Water Res.* 66 (2014) 219-232, <http://dx.doi.org/10.1016/j.waters.2014.08.013>.
- 34 [12] Y.V. Nancharaiyah, S.Venkata Mohan, P.N.L. Lens, Biological and  
35 bioelectrochemical recovery of critical and scarce metals, *Trends Biotechnol.* 34  
36 (2016) 137-155, <http://dx.doi.org/10.1016/j.tibtech.2015.11.003>.
- 37 [13] X. Yong, D. Gu, Y. Wu, Z. Yan, J. Zhou, X. Wu, P. Wei, H. Jia, T. Zheng, Y. Yong,  
38 Bio-electron-fenton (BEF) process driven by microbial fuel cells for triphenyltin  
39 chloride (TPTC) degradation, *J. Hazard. Mater.* 324 (2017) 178-183,  
40 <http://dx.doi.org/10.1016/j.jhazmat.2016.10.047>.
- 41 [14] Q. Zhao, H. Yu, W. Zhang, F.T. Kabutey, J. Jiang, Y. Zhang, K. Wang, J. Ding,  
42 Microbial fuel cell with high content solid wastes as substrates: a review, *Front.*  
43 *Environ. Sci. Eng.* 11 (2017) 13, <http://dx.doi.org/10.1007/s11783-017-0918-6>.
- 44 [15] O. Modin, X. Wang, X. Wu, S. Rauch, K.K. Fedje,

- 1 Bioelectrochemical recovery of Cu, Pb, Cd, and Zn from dilute solutions, *J. Hazard.*  
2 *Mater.* 235 (2012) 291-297, <http://dx.doi.org/10.1016/j.jhazmat.2012.07.058>.
- 3 [16] M. Peiravi, S.R. Mote, M.K. Mohanty, J. Liu, Bioelectrochemical treatment of  
4 acid mine drainage (AMD) from an abandoned coal mine under aerobic condition,  
5 *J. Hazard. Mater.* 333 (2017) 329-338,  
6 <http://dx.doi.org/10.1016/j.jhazmat.2017.03.045>.
- 7 [17] O. Modin, F. Aulenta, Three promising applications of microbial  
8 electrochemistry for the water sector, *Environ. Sci.: Water Res. Technol.* 3 (2017)  
9 391-402, <http://dx.doi.org/10.1039/C6EW00325G>.
- 10 [18] M. Wang, Q. Tan, J.F. Chiang, J. Li, Recovery of rare and precious metals from  
11 urban mines-A review, *Front. Environ. Sci. Eng.* 11 (5) (2017) 1,  
12 <http://dx.doi.org/10.1007/s11783-017-0963-1>.
- 13 [19] B. Zhang, C. Feng, J. Ni, J. Zhang, W. Huang, Simultaneous reduction of  
14 vanadium (V) and chromium (VI) with enhanced energy recovery based on  
15 microbial fuel cell technology, *J. Power Sources* 204 (2012) 34-39,  
16 <http://dx.doi.org/10.1016/j.jpowsour.2012.01.013>.
- 17 [20] H. Luo, G. Liu, R. Zhang, Y. Bai, S. Fu, Y. Hou, Heavy metal recovery combined  
18 with H<sub>2</sub> production from artificial acid mine drainage using the microbial  
19 electrolysis cell, *J. Hazard. Mater.* 270 (2014) 153-159,  
20 <http://dx.doi.org/10.1016/j.jhazmat.2014.01.050>.
- 21 [21] N. Colantonio, Y. Kim, Cadmium (II) removal mechanisms in microbial  
22 electrolysis cells, *J. Hazard. Mater.* 311 (2016) 134-141,  
23 <http://dx.doi.org/10.1016/j.jhazmat.2016.02.062>.
- 24 [22] Y. Li, B. Zhang, M. Cheng, Y. Li, L. Hao, Spontaneous arsenic (III) oxidation  
25 with bioelectricity generation in single-chamber microbial fuel cells, *J. Hazard.*  
26 *Mater.* 306 (2016) 8-12, <http://dx.doi.org/10.1016/j.jhazmat.2015.12.003>.
- 27 [23] Y. Dong, J.F. Liu, M.R. Sui, Y.P. Qu, J.J. Ambuchi, H.M. Wang, Y.J. Feng, A  
28 combined microbial desalination cell and electro dialysis system for  
29 copper-containing wastewater treatment and high-salinity-water desalination, *J.*  
30 *Hazard. Mater.* 321 (2016) 307-315,  
31 <http://dx.doi.org/10.1016/j.jhazmat.2016.08.034>.
- 32 [24] D. Wu, L. Huang, X. Quan, G. Li Puma, Electricity generation and bivalent  
33 copper reduction as a function of operation time and cathode electrode material in  
34 microbial fuel cells, *J. Power Sources* 307 (2016) 705-714,  
35 <https://doi.org/10.1016/j.jpowsour.2016.01.022>.
- 36 [25] R. Qiu, B. Zhang, J. Li, Q. Lv, S. Wang, Q. Gu, Enhanced vanadium (V)  
37 reduction and bioelectricity generation in microbial fuel cells with biocathode, *J.*  
38 *Power Sources* 359 (2017) 379-383,  
39 <http://dx.doi.org/10.1016/j.jpowsour.2017.05.099>.
- 40 [26] G. Wang, B. Zhang, S. Li, M. Yang, C. Yin, Simultaneous microbial reduction of  
41 vanadium (V) and chromium (VI) by *Shewanella loihica* PV-4, *Bioresour. Technol.*  
42 227 (2017) 353-358, <http://dx.doi.org/10.1016/j.jpowsour.2017.05.099>.
- 43 [27] Z. Wang, B. Zhang, Y. Jiang, Y. Li, C. He, Spontaneous thallium (I) oxidation  
44 with electricity generation in single-chamber microbial fuel cells, *Appl. Energy* 209  
45

(2018) 33-42, <http://dx.doi.org/10.1016/j.apenergy.2017.10.075>.

- [28] J. Shen, Y. Sun, L. Huang, J. Yang, Microbial electrolysis cells with biocathodes and driven by microbial fuel cells for simultaneous enhanced Co(II) and Cu(II) removal, *Front. Environ. Sci. Eng.* 9 (2015) 1084-1095, <http://dx.doi.org/10.1007/s11783-015-0805-y>.
- [29] Y. Zhang, L. Yu, D. Wu, L. Huang, P. Zhou, X. Quan, G. Chen, Dependency of simultaneous Cr(VI), Cu(II) and Cd(II) reduction on the cathodes of microbial electrolysis cells self-driven by microbial fuel cells, *J. Power Sources* 273 (2015) 1103-1113, <https://doi.org/10.1016/j.jpowsour.2014.09.126>.
- [30] D. Wu, Y. Pan, L. Huang, X. Quan, J. Yang, Comparison of Co(II) reduction on three different cathodes of microbial electrolysis cells driven by Cu(II)-reduced microbial fuel cells under various cathode volume conditions, *Chem. Eng. J.* 266 (2015) 121-132, <https://doi.org/10.1016/j.cej.2014.12.078>.
- [31] D. Wu, Y. Pan, L. Huang, P. Zhou, X. Quan, H. Chen, Complete separation of Cu(II), Co(II) and Li(I) using self-driven MFCs-MECs with stainless steel mesh cathodes under continuous flow conditions, *Sep. Purif. Technol.* 147 (2015) 114-124, <http://dx.doi.org/10.1016/j.seppur.2015.04.016>.
- [32] M. Li, Y. Pan, L. Huang, Y. Zhang, J. Yang, Continuous flow operation with appropriately adjusting composites in influent for recovery of Cr(VI), Cu(II) and Cd(II) in self-driven MFC-MEC system, *Environ. Technol.* 38 (2017) 615-628, <http://dx.doi.org/10.1080/09593330.2016.1205149>.
- [33] N.A. Abdel Ghany, S. Meguro, N. Kumagai, K. Asami, K. Hashimoto, Adodically deposited Mn-Mo-Fe oxide anodes for oxygen evolution in hot seawater electrolysis, *Mater. Trans.* 44 (2003) 2114-2123.
- [34] Y. Ruiz, J.A. Baeza, A. Guisasola, Enhanced performance of bioelectrochemical hydrogen production using a pH control strategy, *ChemSusChem* 8 (2015) 389-397, <http://dx.doi.org/10.1002/cssc.201403083>.
- [35] A. Kadier, M. Sahaid Kalil, P. Abdeshahian, K. Chandrasekhar, A. Mohamed, N. Farhana Azman, W. Logroño, Y. Simayi, A. Abdul Hamid, Recent advances and emerging challenges in microbial electrolysis cells (MECs) for microbial production of hydrogen and value-added chemicals, *Renew. Sust. Energ. Rev.* 61 (2016) 501-525, <https://doi.org/10.1016/j.rser.2016.04.017>.
- [36] L. Huang, B. Yao, D. Wu, X. Quan, Complete cobalt recovery from lithium cobalt oxide in self-driven microbial fuel cell-microbial electrolysis cell systems, *J. Power Sources* 259 (2014) 54-64, <https://doi.org/10.1016/j.jpowsour.2014.02.061>.
- [37] Q. Wang, L. Huang, H. Yu, X. Quan, Y. Li, G. Fan, L. Li, Assessment of five different cathode materials for Co(II) reduction with simultaneous hydrogen evolution in microbial electrolysis cells, *Inter. J. Hydrogen Energy* 40 (2015) 184-196, <https://doi.org/10.1016/j.ijhydene.2014.11.014>.
- [38] Q. Wang, L. Huang, Y. Pan, P. Zhou, X. Quan, B.E. Logan, H. Chen, Cooperative cathode electrode and in situ deposited copper for subsequent enhanced Cd(II) removal and hydrogen evolution in bioelectrochemical systems, *Bioresour. Technol.* 200 (2016) 565-571, <https://doi.org/10.1016/j.biortech.2015.10.084>.
- [39] Q. Wang, L. Huang, Y. Pan, X. Quan, G. Li Puma, Impact of Fe(III) as an

1 effective mediator for enhanced Cr(VI) reduction in microbial fuel cells: Reduction  
2 of diffusional resistances and cathode overpotentials, *J. Hazard. Mater.* 321 (2017)  
3 896-906, <http://dx.doi.org/10.1016/j.jhazmat.2016.10.011>.

4 [40] N. Tsyntsar, H. Cesiulis, M. Donten, J. Sort, E. Pellicer, E.J. Podlaha-Murphy,  
5 Modern trends in tungsten alloys electrodeposition with iron group metals, *Surface*  
6 *Eng. Appl. Electrochem.* 48 (2012) 491-520,  
7 <http://dx.doi.org/10.3103/S1068375512060038>.

8 [41] T.G. Kelly, S.T. Hunt, D.V. Esposito, J.G. Chen, Monolayer palladium supported  
9 on molybdenum and tungsten carbide substrates as low-cost hydrogen evolution  
10 reaction (HER) electrocatalysts, *Inter. J. Hydrogen Energy* 38 (2013) 5638-5644,  
11 <https://doi.org/10.1016/j.ijhydene.2013.02.116>.

12 [42] M. Zhang, D. Lu, G. Yan, J. Wu, J. Yang, Fabrication of Mo+N-codoped TiO<sub>2</sub>  
13 nanotube arrays by anodization and sputtering for visible light-induced  
14 photoelectrochemical and photocatalytic properties, *J. Nanomater.* 2013 (2013) 1-9,  
15 <http://dx.doi.org/10.1155/2013/648346>.

16 [43] Q. Wang, L. Huang, X. Quan, Q. Zhao, Preferable utilization of in-situ produced  
17 H<sub>2</sub>O<sub>2</sub> rather than externally added for efficient deposition of tungsten and  
18 molybdenum in microbial fuel cells, *Electrochim. Acta* 247C (2017) 880-890,  
19 <https://doi.org/10.1016/j.electacta.2017.07.079>.

20 [44] Y. Chen, J. Shen, L. Huang, Y. Pan, X. Quan, Enhanced Cd(II) removal with  
21 simultaneous hydrogen production in biocathode microbial electrolysis cells in the  
22 presence of acetate or NaHCO<sub>3</sub>, *Inter. J. Hydrogen Energy* 41 (2016) 13368-13379,  
23 <https://doi.org/10.1016/j.ijhydene.2016.06.200>.

24 [45] B.E. Logan, Essential data and techniques for conducting microbial fuel cell and  
25 other types of bioelectrochemical system experiments, *ChemSusChem* 5 (2012)  
26 988-994, <https://doi.org/10.1002/cssc.201100604>.

27 [46] American Public Health Association, American Water Works Association, Water  
28 Pollution Control Federation, Standard methods for the examination of water and  
29 wastewater, 20th edn. American Public Health Association, Washington, 1998.

30 [47] Z. He, F. Mansfeld, Exploring the use of electrochemical impedance  
31 spectroscopy (EIS) in microbial fuel cell studies, *Energy Environ. Sci.* 2 (2009)  
32 215-219, <https://doi.org/10.1039/B814914C>.

33 [48] V. Madhavi, P. Jeevan Kumar, P. Kondaiah, O.M. Hussain, S. Uthanna, Effect of  
34 molybdenum doping on the electrochromic properties of tungsten oxide thin films  
35 by RF magnetron sputtering, *Ionics* 20 (2014) 1737-1745,  
36 <https://doi.org/10.1007/s11581-014-1073-8>.

37 [49] I. Andersson, J.J. Hastings, O.W. Howarth, L. Pettersson, Aqueous  
38 molybdotungstates, *J. Chem. Soc. Dalton Trans.* (1994) 1061-1066,  
39 <https://doi.org/10.1039/DT9940001061>.

40 [50] A. Katrib, V. Logie, N. Saurel, P. Wehrer, L. Hilaire, G. Maire, Surface electronic  
41 structure and isomerization reactions of alkanes on some transition metal oxides,  
42 *Surf. Sci.* 377 (1997) 754-758, [https://doi.org/S0039-6028\(96\)01488-4](https://doi.org/S0039-6028(96)01488-4).

43 [51] L. Huang, L. Gan, N. Wang, X. Quan, B.E. Logan, G. Chen, Mineralization of  
44 pentachlorophenol with enhanced degradation and power generation from air  
45  
46  
47  
48  
49  
50  
51  
52  
53  
54  
55  
56  
57  
58  
59  
60  
61  
62  
63  
64  
65

cathode microbial fuel cells, *Biotechnol. Bioeng.* 109 (2012) 2211-2221, <https://doi.org/10.1002/bit.24489>.

[52] L. Cao, W. Sun, Y. Zhang, S. Feng, J. Dong, Y. Zhang, B.E. Rittmann, Competition for electrons between reductive dechlorination and denitrification, *Front. Environ. Sci. Eng.* 11 (2017) 14, <https://doi.org/10.1007/s11783-017-0959-x>.

[53] F. Jiang, Y. Zhang, N. Sun, Z. Liu, Effect of direct current density on microstructure of tungsten coating electroplated from  $\text{Na}_2\text{WO}_4\text{-WO}_3\text{-NaPO}_3$  system, *Appl. Surface Sci.* 317 (2014) 867-874, <https://doi.org/10.1016/j.apsusc.2014.09.031>.

[54] W. Li, H. Yu, Z. He, Towards sustainable wastewater treatment by using microbial fuel cell-centered technologies, *Energy Environ. Sci.* 7 (2014) 911-924, <https://doi.org/10.1039/C3EE43106A>.

[55] D. Jafarifar, M.R. Daryanavard, S. Sheibani, Ultra fast microwave-assisted leaching for recovery of platinum from spent catalyst, *Hydrometallurgy* 78 (2005) 166-171, <https://doi.org/10.1016/j.hydromet.2005.02.006>.

[56] H.L. Le, J. Jeong, J.C. Lee, B.D. Pandey, J.M. Yoo, T.H. Huynh, Hydrometallurgical process for copper recovery from waste printed circuit boards (PCBs), *Miner. Process. Extr. Metall. Rev.* 32 (2011) 90-104, <https://doi.org/10.1080/08827508.2010.530720>.

**Table 1** Separator factors in the 1# and the 2# units under various operational conditions

**Fig. 1** Effect of various W concentrations on rates of (A) W and (B) Mo deposition, (D) current, and (E) cathode potential in the stacked BESs. (C) Applied voltage and (F) hydrogen production in the 1# unit of the stacked BESs. (initial Mo(VI) fixed at 1.0 mM, initial pH: 2.0, cathode: SSS in the 1# and CR in the 2# units).

**Fig. 2** Effect of various Mo concentrations on rates of (A) W and (B) Mo deposition, (C) current, (D) cathode potential, (E) applied voltage, and (F) hydrogen production in the stacked BESs (initial W(VI) fixed at 1.0 mM, initial pH: 2.0, cathode: SSS in the 1# and CR in the 2# units).

**Fig. 3** XPS analysis for (A, C, E and G) W and (B, D, F and H) Mo elements on the cathodes of (A, B, E and F) the 1# and (C, D, G and H) the 2# units at W/Mo molar ratios of (A, B, C and D) 1 : 0.01 or (E, F, G and H) 0.01 : 1 (initial pH: 2.0, cathode: SSS in the 1# and CR in the 2# units).

**Fig. 4** EIS analysis at W/Mo molar ratios of (A) 1 : 1, 0.1 : 1, 0.05 : 1 and 0.01 : 1, and (B) 1 : 0.01, 1 : 0.05, 1 : 0.1 and 1 : 1 as well as (C) single W or Mo (initial pH: 2.0, cathode: SSS in the 1# and CR in the 2# units).

**Fig. 5** Effect of initial pHs on rates of (A) W and (B) Mo deposition, (C) current, (D) cathode potential, (E) applied voltage and (F) hydrogen production in the stacked BESs (W : Mo = 1 : 1; cathode: SSS in the 1# and CR in the 2# units).

**Fig. 6** XPS analysis for (A, C, E and G) W and (B, D, F and H) Mo elements on the cathodes of (A, B, C and D) the 1# and (E, F, G and H) the 2# units at an initial pH of (A, B, E and F) 1.5 or (C, D, G and H) 4.0 (W : Mo = 1 : 1, cathode: SSS in the 1# and CR in the 2# units).



**Fig. 7** Effect of cathode material on rates of (A) W and (B) Mo deposition, (C) current, (D) cathode potential and (E) applied voltage in the stacked BESs. (F) Rate of hydrogen production in the 1# unit of the stacked BESs (W : Mo = 1 : 1; initial pH: 2.0).

**Fig. 8** Rates of (A) W and (B) Mo deposition, (C) current, (D) cathode potential, (E) applied voltage and (F) hydrogen production as a function of equal W/Mo molar ratio (CR in the 1# unit and SSS in the 2 units, initial pH: 2.0).

**Statement of novelty**

W/Mo molar ratio (in the range 0.01 mM : 1 mM and vice-versa), initial pH (1.5 to 4.0), and cathode material (stainless steel mesh, carbon rod and titanium sheet) were revealed for the first time to dramatically impact performance of stacked bioelectrochemical systems composed of microbial electrolysis cell (MEC) serially connected with parallel connected microbial fuel cell (MFC). These impacts were ascribed to the changes in circuital current, cathode potential, voltage output from the MFC applied to the MEC, diffusional resistance and cathode overpotential. Complete metal recovery was achieved at equimolar W/Mo ratio of 0.05 mM : 0.05 mM.

- Concentration of Mo(VI) more influential than W(VI) on system performance;
- Complete metal recovery was achieved at equimolar W/Mo ratio of 0.05 mM :  
0.05 mM;
- Acidic pH favored the rates of metal deposition and hydrogen production;
- Stainless steel mesh, carbon rod and titanium sheet cathodes impacted performance.

**Abstract:** The deposition and separation of W and Mo from aqueous solutions with simultaneous hydrogen production was investigated in stacked bioelectrochemical systems (BESs) composed of microbial electrolysis cell (1#) serially connected with parallel connected microbial fuel cell (2#). The impact of W/Mo molar ratio (in the range 0.01 mM : 1 mM and vice-versa), initial pH (1.5 to 4.0) and cathode material (stainless steel mesh (SSM), carbon rod (CR) and titanium sheet (TS)) on the BES performance was systematically investigated. The concentration of Mo(VI) was more influential than W(VI) in determining the rate of deposition of both metals and the rate of hydrogen production. Complete metal recovery was achieved at equimolar W/Mo ratio of 0.05 mM : 0.05 mM. The rates of metal deposition and hydrogen production increased at acidic pH, with the fastest rates at pH 1.5. The morphology of the metal deposits and the valence of the Mo were correlated with W/Mo ratio and pH. CR cathodes (2#) coupled with SSM cathodes (1#) achieved a significant rate of hydrogen production ( $0.82 \pm 0.04 \text{ m}^3/\text{m}^3/\text{d}$ ) with W and Mo deposition ( $0.049 \pm 0.003 \text{ mmol/L/h}$  and  $0.140 \pm 0.004 \text{ mmol/L/h}$  (1#);  $0.025 \pm 0.001 \text{ mmol/L/h}$  and  $0.090 \pm 0.006 \text{ mmol/L/h}$  (2#)).

**Keywords:** Bioelectrochemical system; microbial fuel cell; microbial electrolysis cells; W and Mo deposition; hydrogen production

**Table 1****Table 1** Separator factors in the 1# and the 2# units under various operational conditions

	W/Mo molar ratio						
	1 : 0.01	1 : 0.05	1 : 0.1	1 : 1	0.1 : 1	0.05 : 1	0.01 : 1
1#	$\infty$	$939 \pm 20$	$717 \pm 4$	$7.4 \pm 0.1$	$5.2 \pm 0.8$	$3.8 \pm 0.3$	---
2#	$\infty$	$605 \pm 10$	$200 \pm 8$	$4.9 \pm 0.1$	$3.3 \pm 0.2$	$2.4 \pm 0.1$	---
	Initial pH						
	1.5	2.0	2.5	3.0	3.5	4.0	
1#	$6.7 \pm 0.8$	$7.4 \pm 0.1$	$5.3 \pm 0.3$	$4.2 \pm 0.2$	$3.1 \pm 0.2$	$2.3 \pm 0.3$	
2#	$4.8 \pm 0.5$	$4.9 \pm 0.1$	$4.5 \pm 0.3$	$3.1 \pm 0.1$	$2.9 \pm 0.0$	$2.1 \pm 0.0$	
	Cathode material						
	CR-CR	CR-SSS	CR-Ti	SSS-SSS			
1#	$4.1 \pm 0.7$	$5.2 \pm 0.8$	$5.7 \pm 1.1$	$7.4 \pm 0.1$			
2#	$4.2 \pm 0.1$	$5.0 \pm 0.4$	$4.7 \pm 1.0$	$4.9 \pm 0.0$			
	W/Mo molar ratio						
	1 : 1	0.1 : 0.1	0.05 : 0.05				
1#	$5.2 \pm 0.4$	$5.6 \pm 2.3$	$1.6 \pm 0.2$				
2#	$5.0 \pm 0.2$	$2.2 \pm 0.1$	$3.7 \pm 0.1$				

Figure 1  
[Click here to download high resolution image](#)

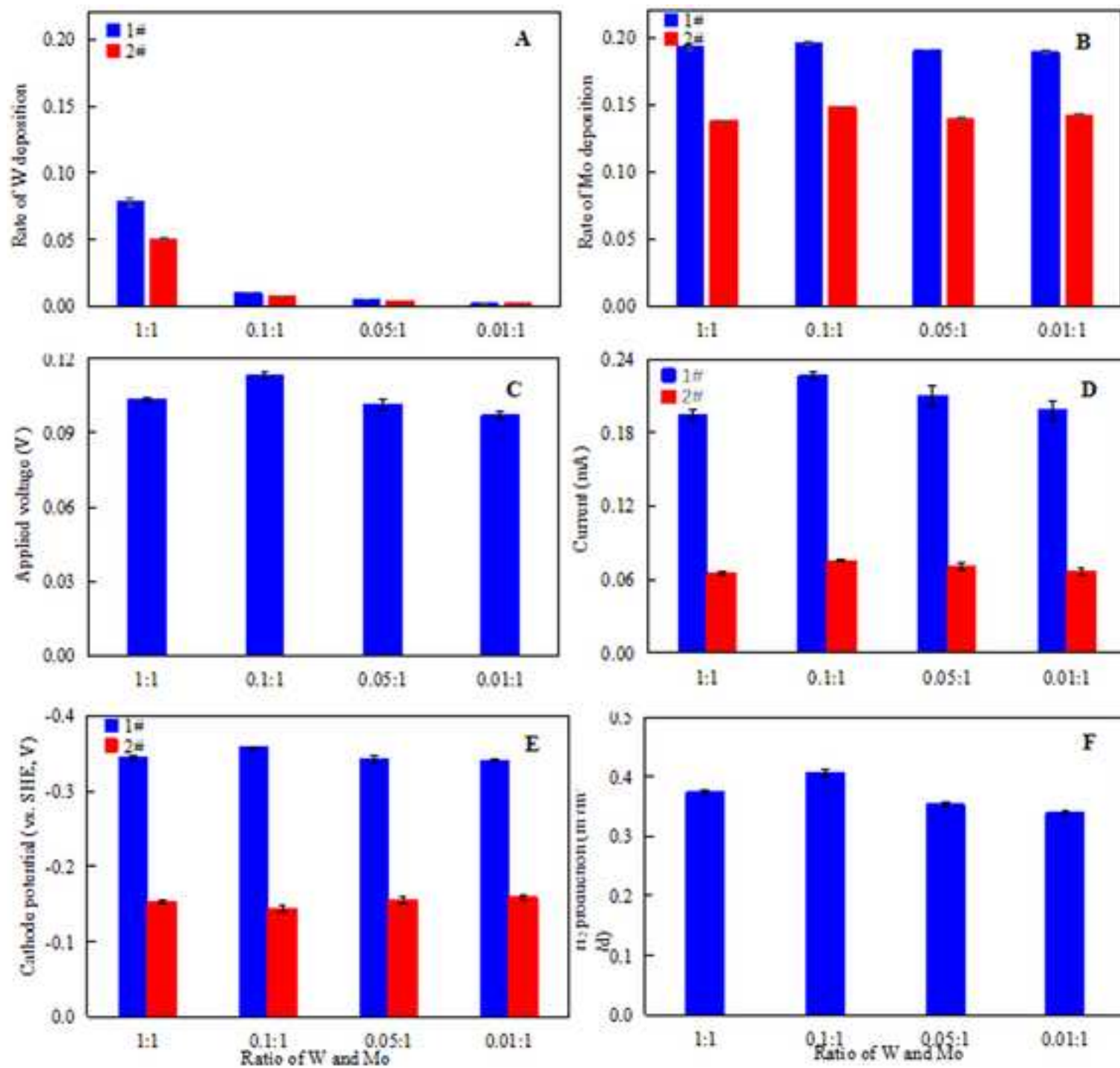


Figure 2

[Click here to download high resolution image](#)

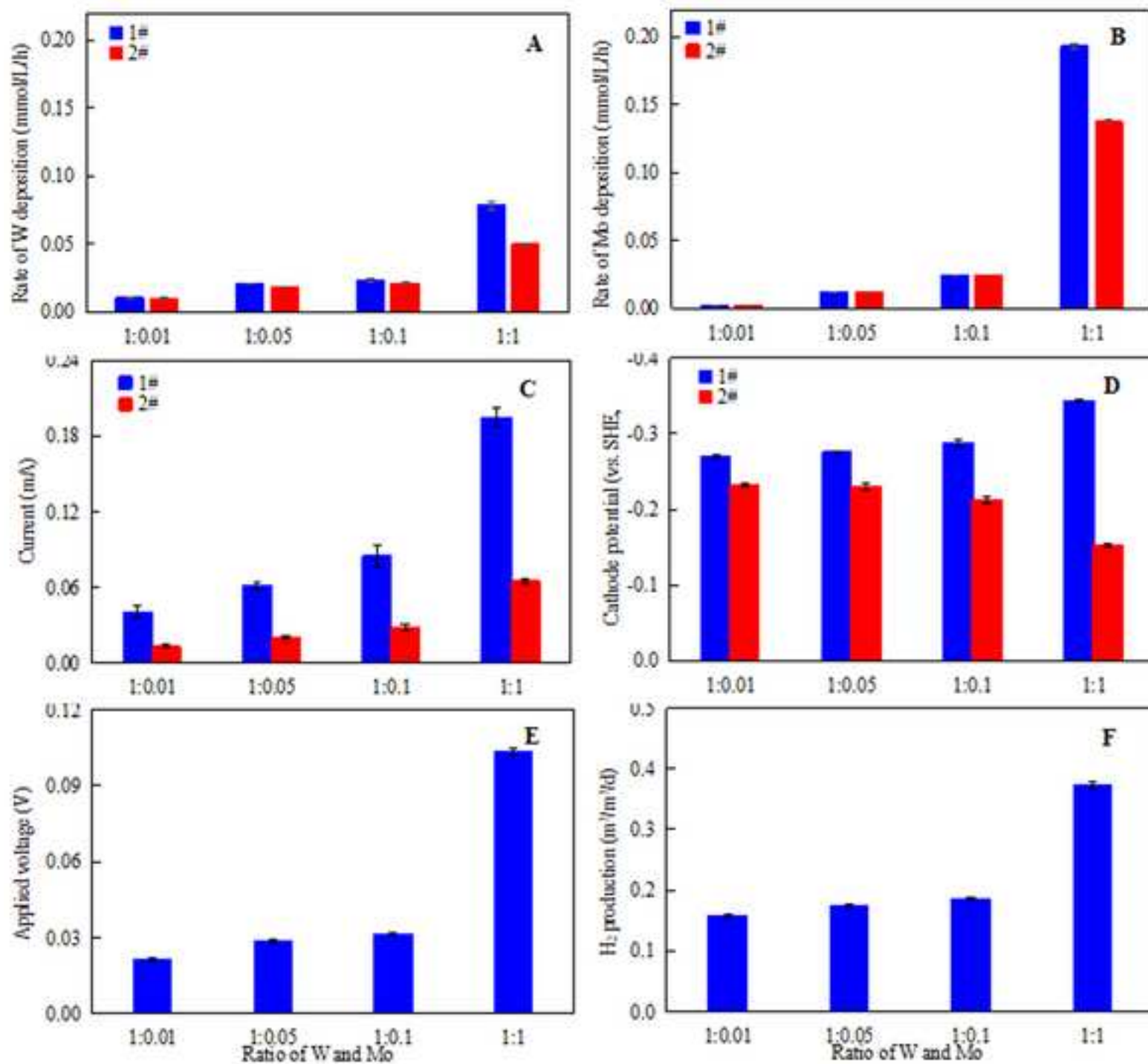


Figure 3  
[Click here to download high resolution image](#)

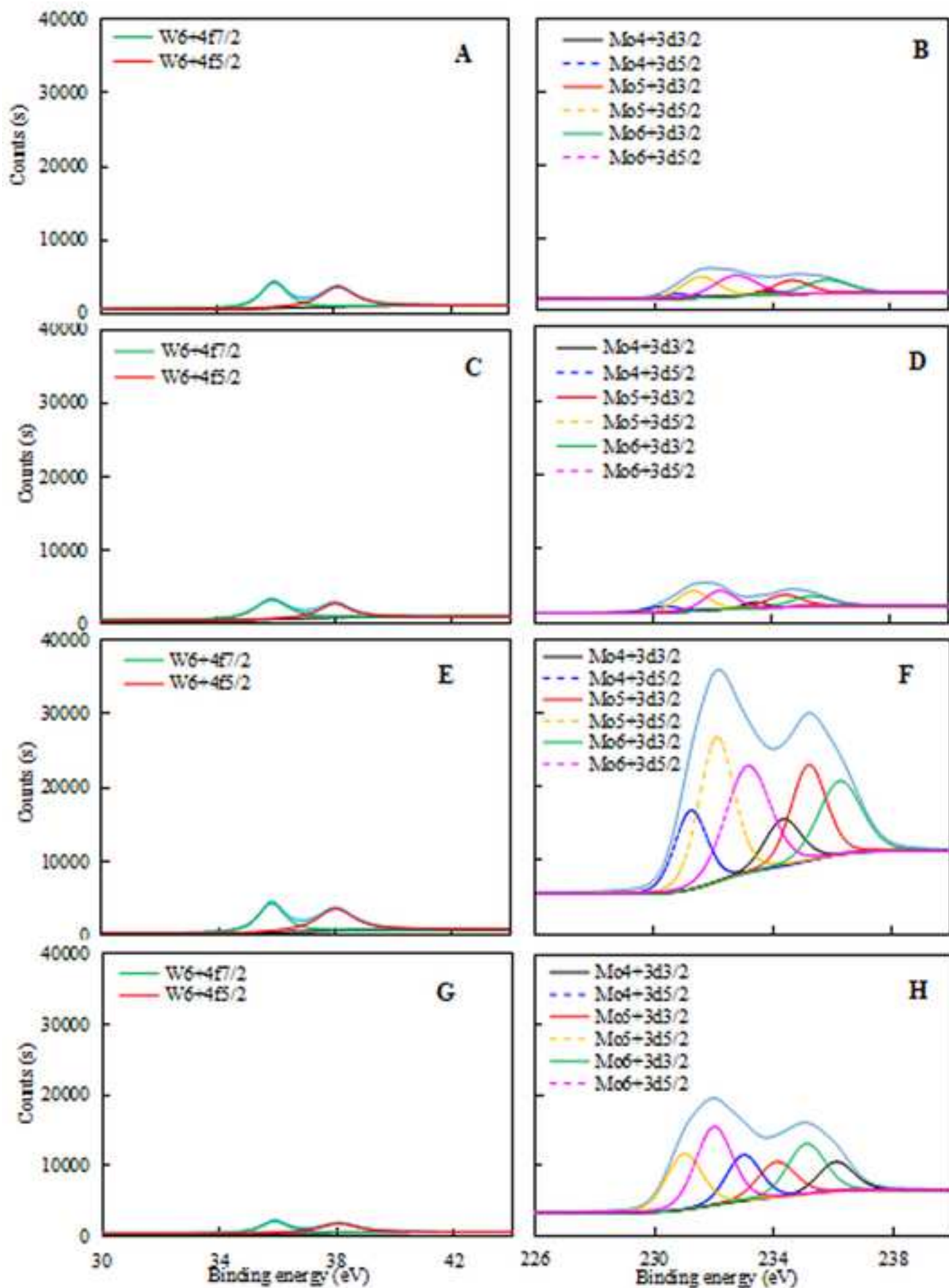




Figure 4

[Click here to download high resolution image](#)

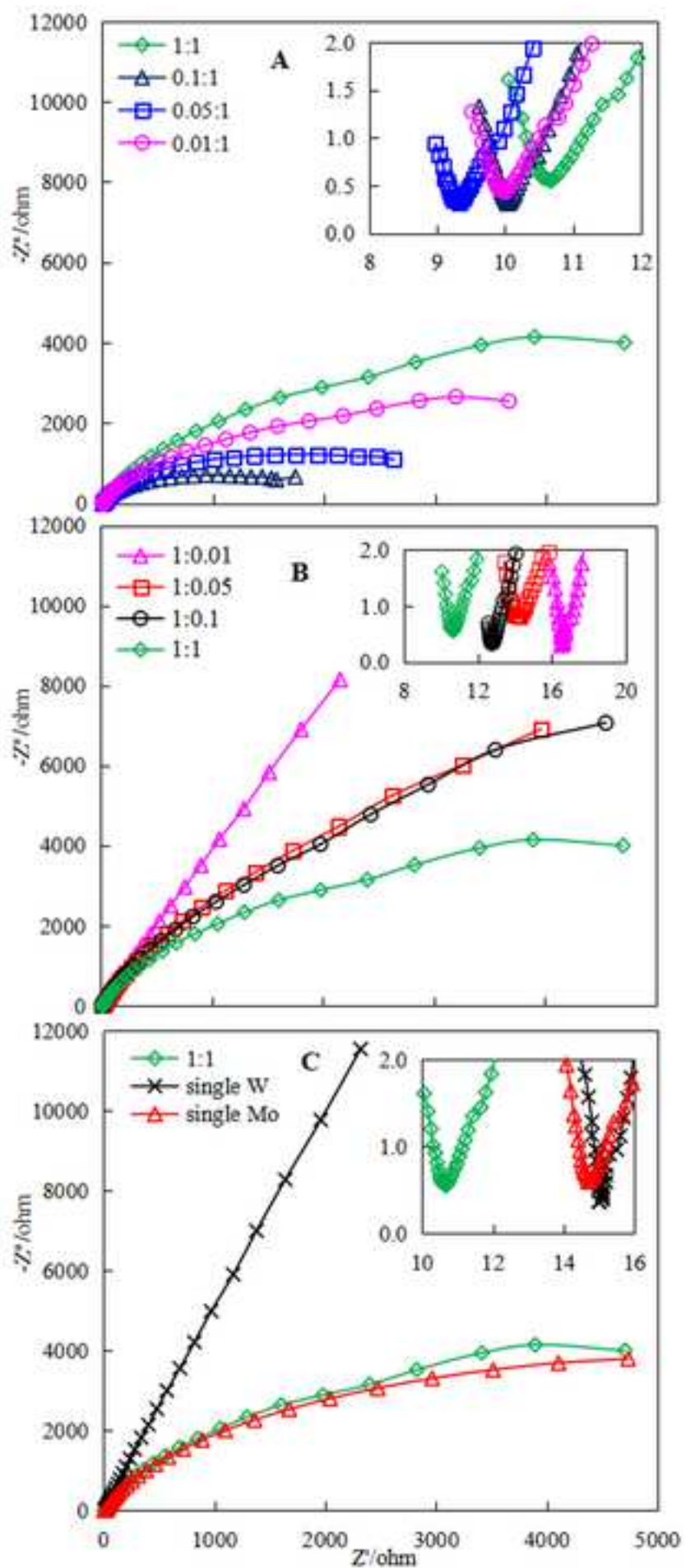


Figure 5  
[Click here to download high resolution image](#)

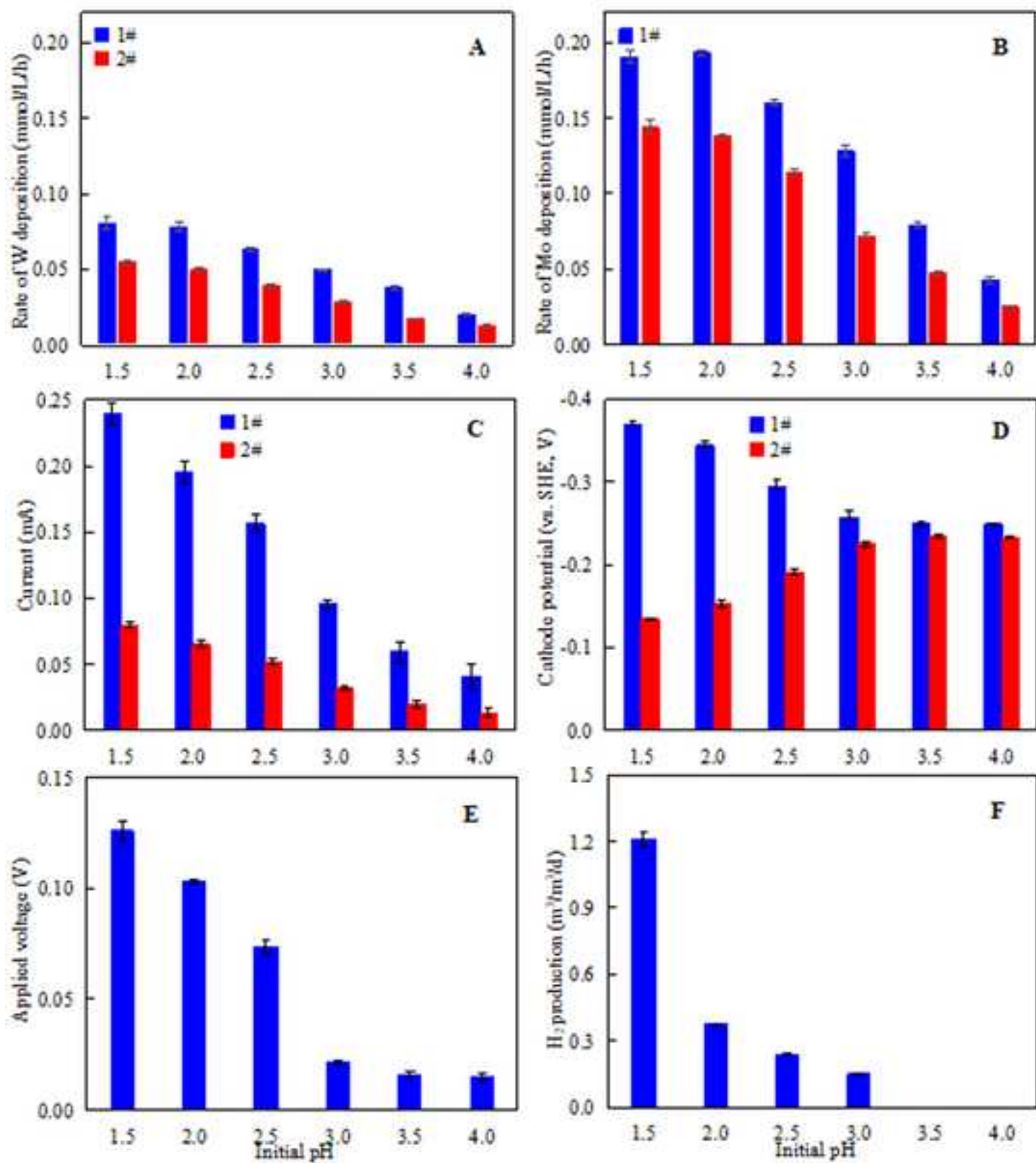
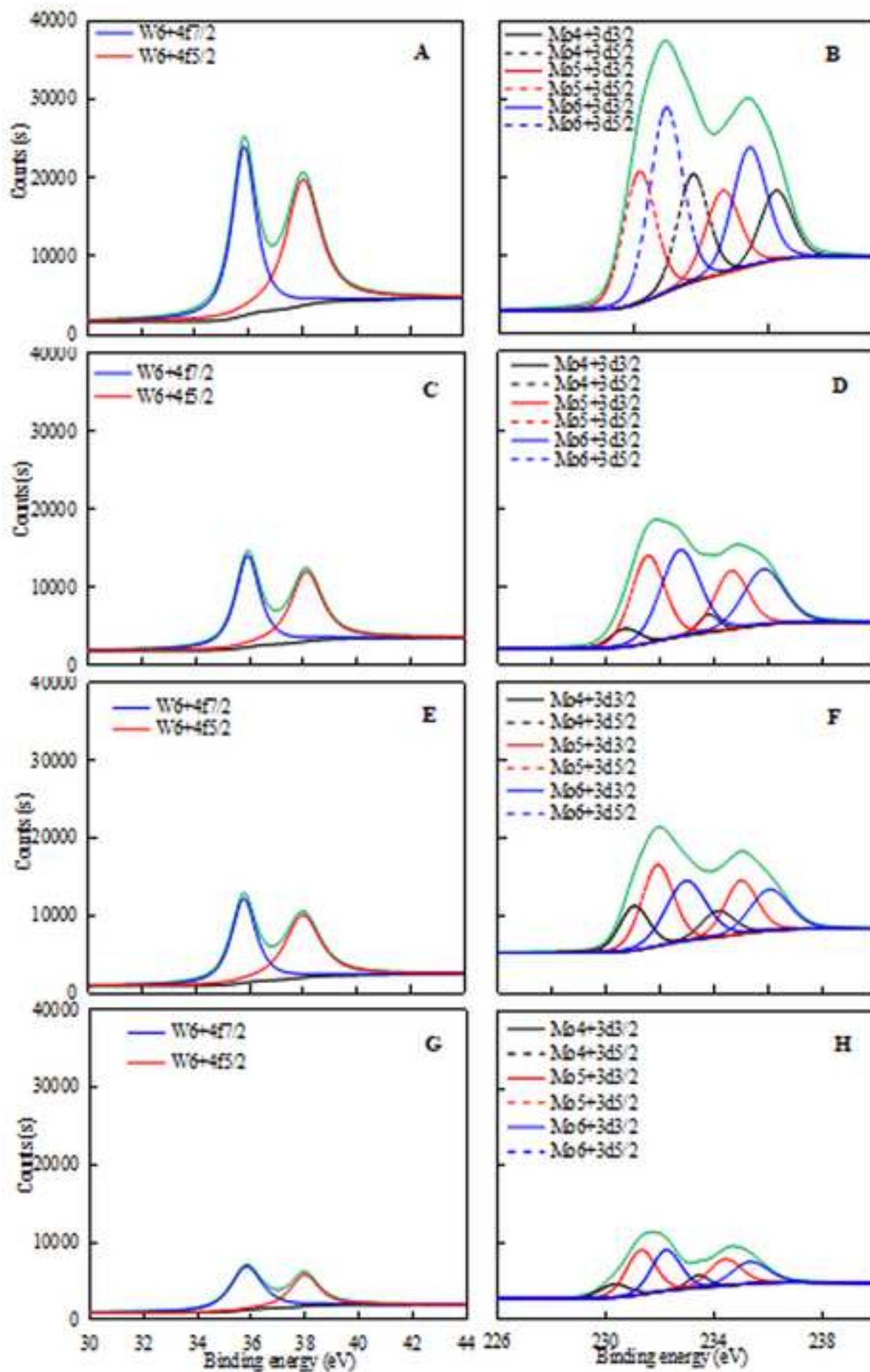


Figure 6  
[Click here to download high resolution image](#)



**Figure 7**  
[Click here to download high resolution image](#)

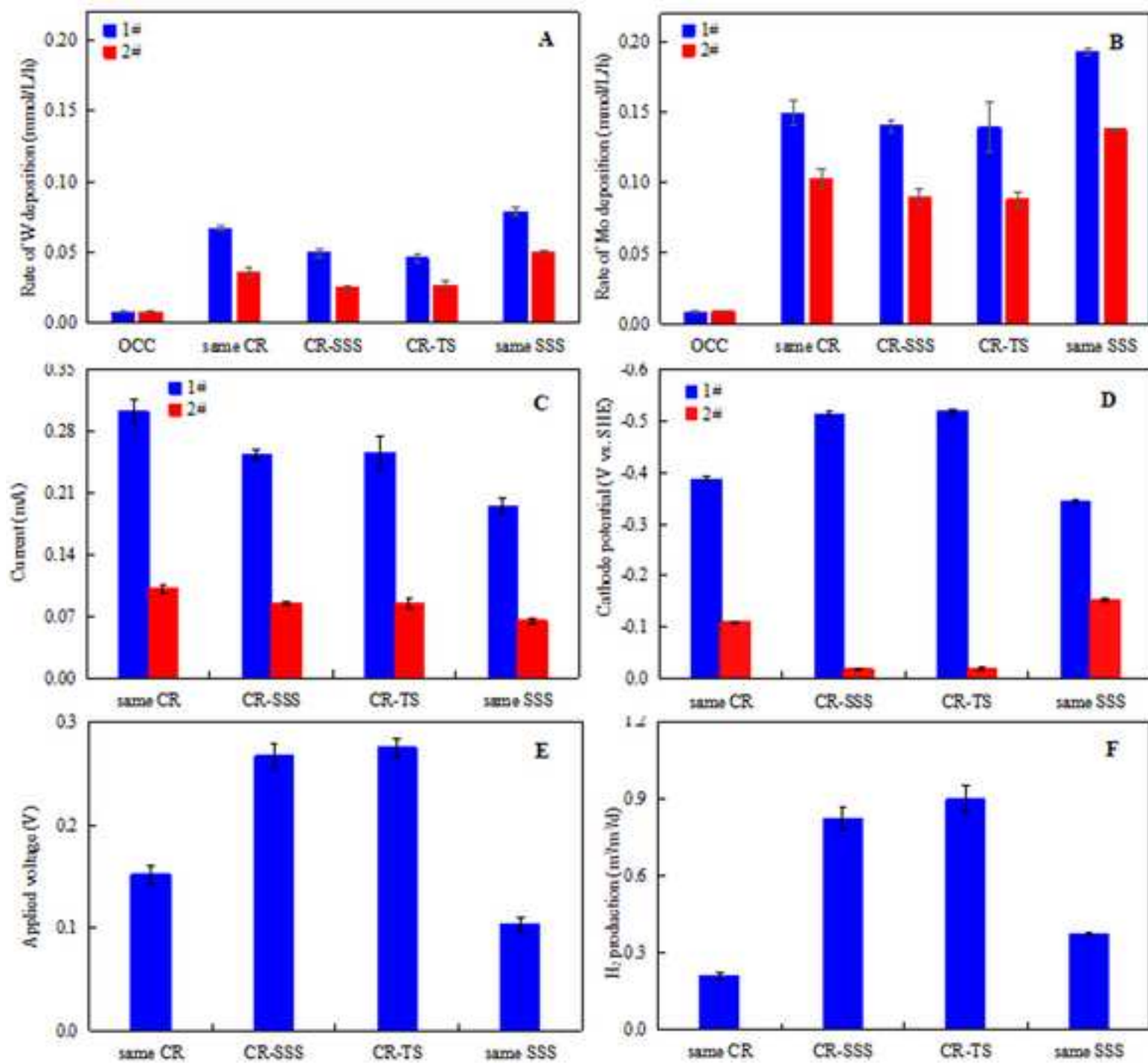
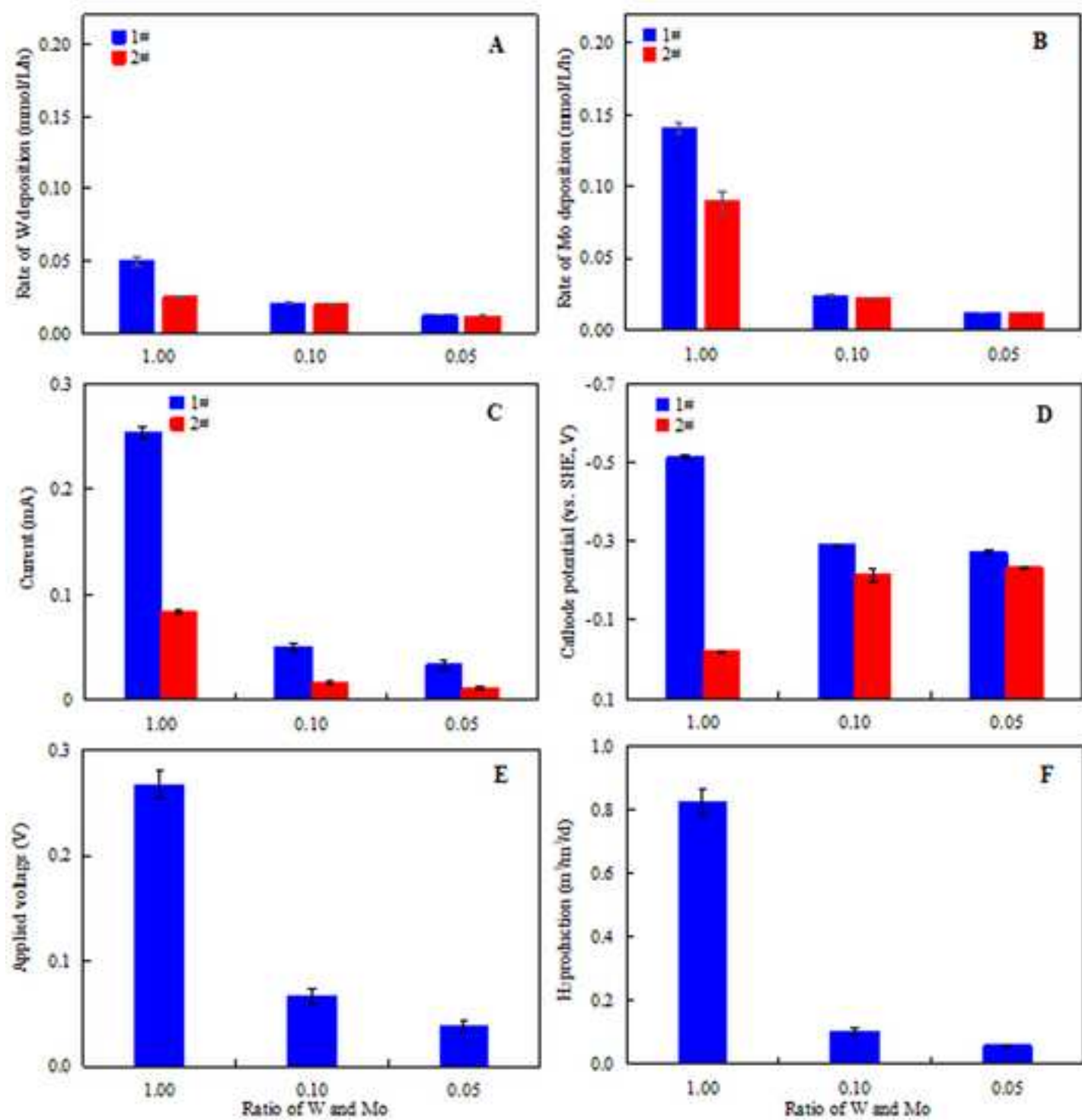


Figure 8  
[Click here to download high resolution image](#)



*Supplementary Material*

**Deposition and separation of W and Mo from aqueous solutions with simultaneous hydrogen production in stacked bioelectrochemical systems (BESs): Impact of heavy metals W(VI)/Mo(VI) molar ratio, initial pH and electrode material**

Liping Huang<sup>1,\*</sup>, Ming Li<sup>1</sup>, Yuzhen Pan<sup>2</sup>, Xie Quan<sup>1</sup>, Jinhui Yang<sup>2</sup>, Gianluca Li Puma<sup>3,\*</sup>

1. Key Laboratory of Industrial Ecology and Environmental Engineering, Ministry of Education (MOE), School of Environmental Science and Technology, Dalian University of Technology, Dalian 116024, China

2. College of Chemistry, Dalian University of Technology, Dalian 116024, China

3. Environmental Nanocatalysis & Photoreaction Engineering, Department of Chemical Engineering, Loughborough University, Loughborough LE11 3TU, United Kingdom

**Corresponding authors:**

(L. Huang) [lipinghuang@dlut.edu.cn](mailto:lipinghuang@dlut.edu.cn)

(G. Li Puma) [g.lipuma@lboro.ac.uk](mailto:g.lipuma@lboro.ac.uk)

The authors declare no competing financial interest.

Pages: 13

Tables: 2

Figures: 9

## S2 Materials and Methods

### S2.1 Measurements and analyses

$$R_w = \frac{W(VI)_0 - W(VI)_t}{t} \quad (S1)$$

$$R_{Mo} = \frac{Mo(VI)_0 - Mo(VI)_t}{t} \quad (S2)$$

$$R_{H_2} = \frac{24 \times \eta_{H_2}}{t} \quad (S3)$$

$$\varepsilon = \frac{Mo(VI)_0 - Mo(VI)_t}{Mo(VI)_0} \times \frac{W(VI)_t}{W(VI)_0 - W(VI)_t} \quad (S4)$$

where  $W(VI)_0$  and  $Mo(VI)_0$  are the initial concentrations (mmol/L) of W(VI) and Mo(VI) in the catholyte of each unit, respectively, and the subscript  $t$  refers to the concentration after an operational time of  $t$  (h).  $\eta_{H_2}$  is the hydrogen concentration ( $m^3/m^3$ ) at  $t$  hours.

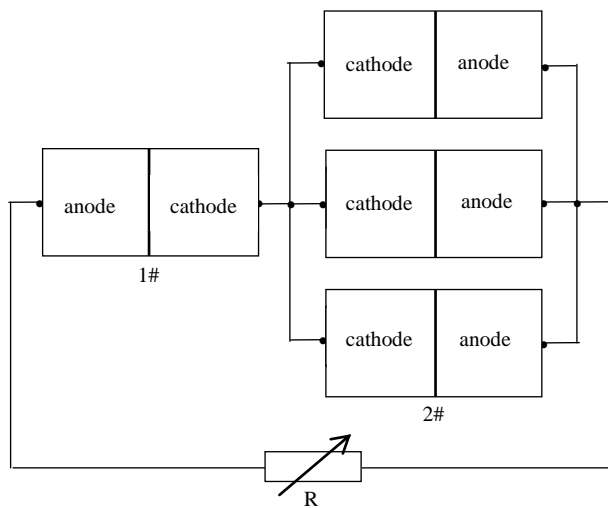


**Fig. S1** Schematic diagram of stacked BESs



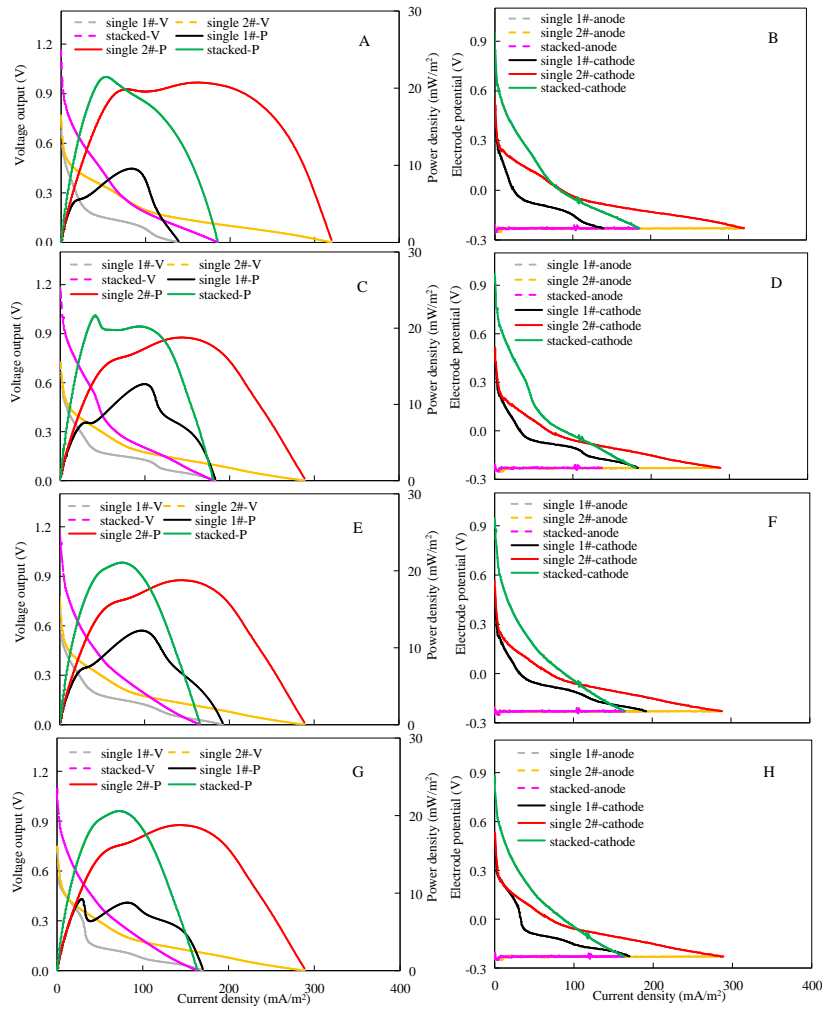


**Fig. S2** (A, C, E and G) Polarization curves and (B, D, F and H) electrode potentials of the stacked BESs under various W/Mo molar ratios of (A and B) 1 : 1, (C and D) 0.1 : 1, (E and F) 0.05 : 1, and (G and H) 0.01 : 1.

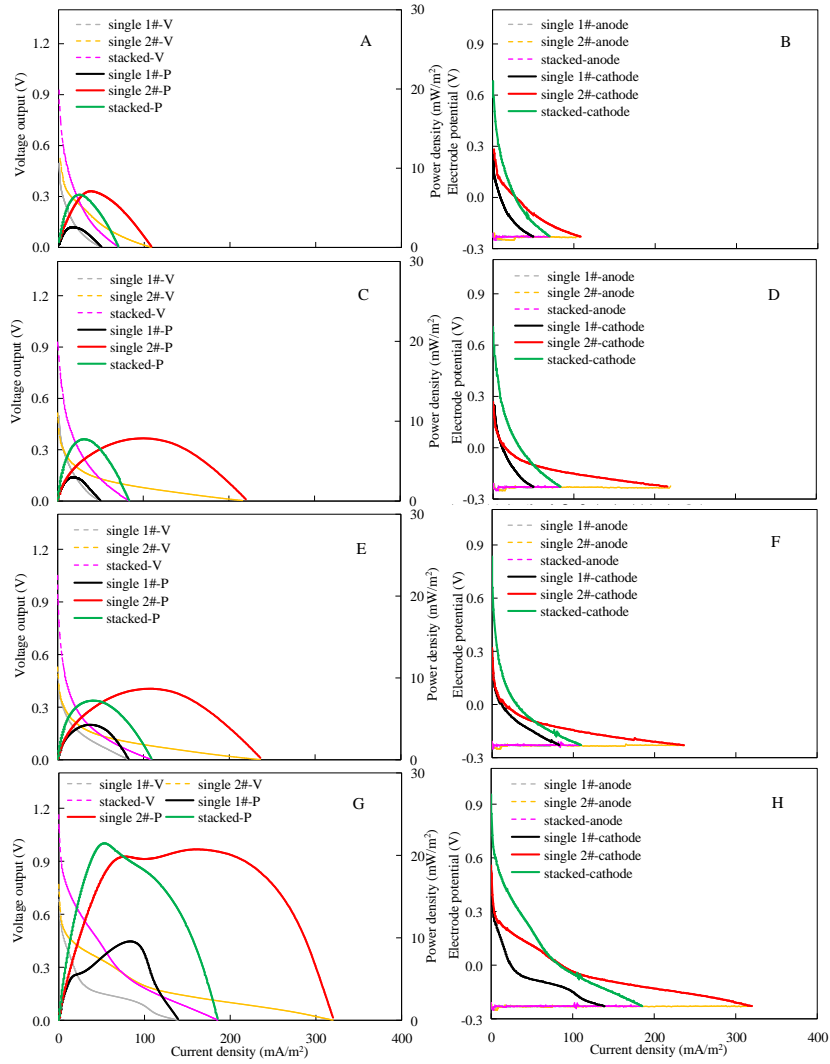


**Fig. S3** (A, C, E and G) Polarization curves and (B, D, F and H) electrode potentials of the stacked BESs at various W/Mo molar ratios of (A and B) 1 : 0.01, (C and D) 1 : 0.05, (E and F) 1 : 0.1, and (G and H) 1 : 1.

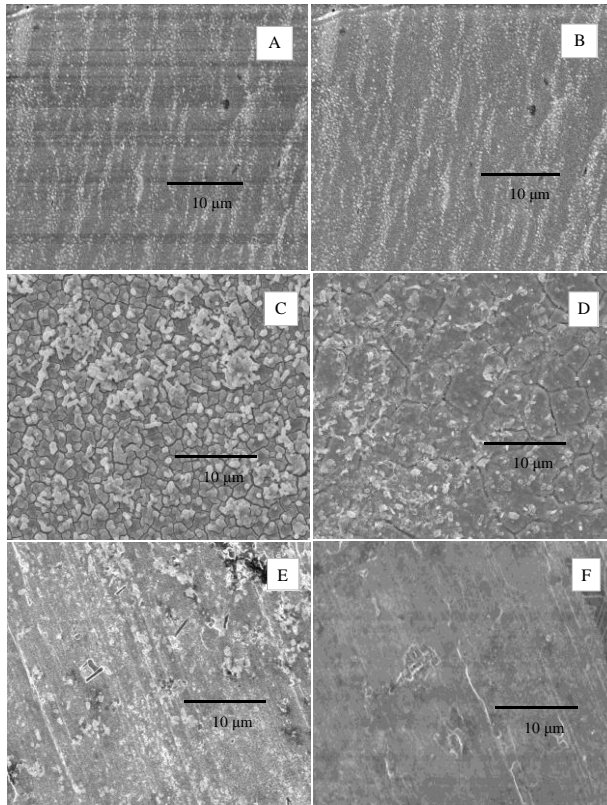


**Fig. S4** Morphology of W and Mo deposition on (A, C and E) the 1# unit and (B, D and F) the 2# units of the stacked BESs under W/Mo molar ratios of (A and B) 1 : 0.01, (C and D) 1 : 1, and (E and F) 0.01 : 1.

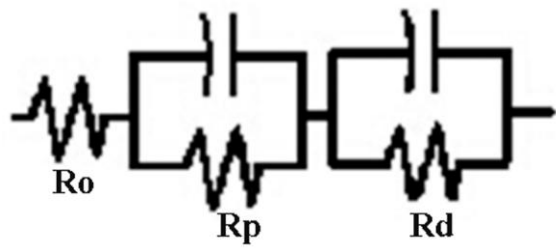


**Fig. S5** EIS equivalent circuits.



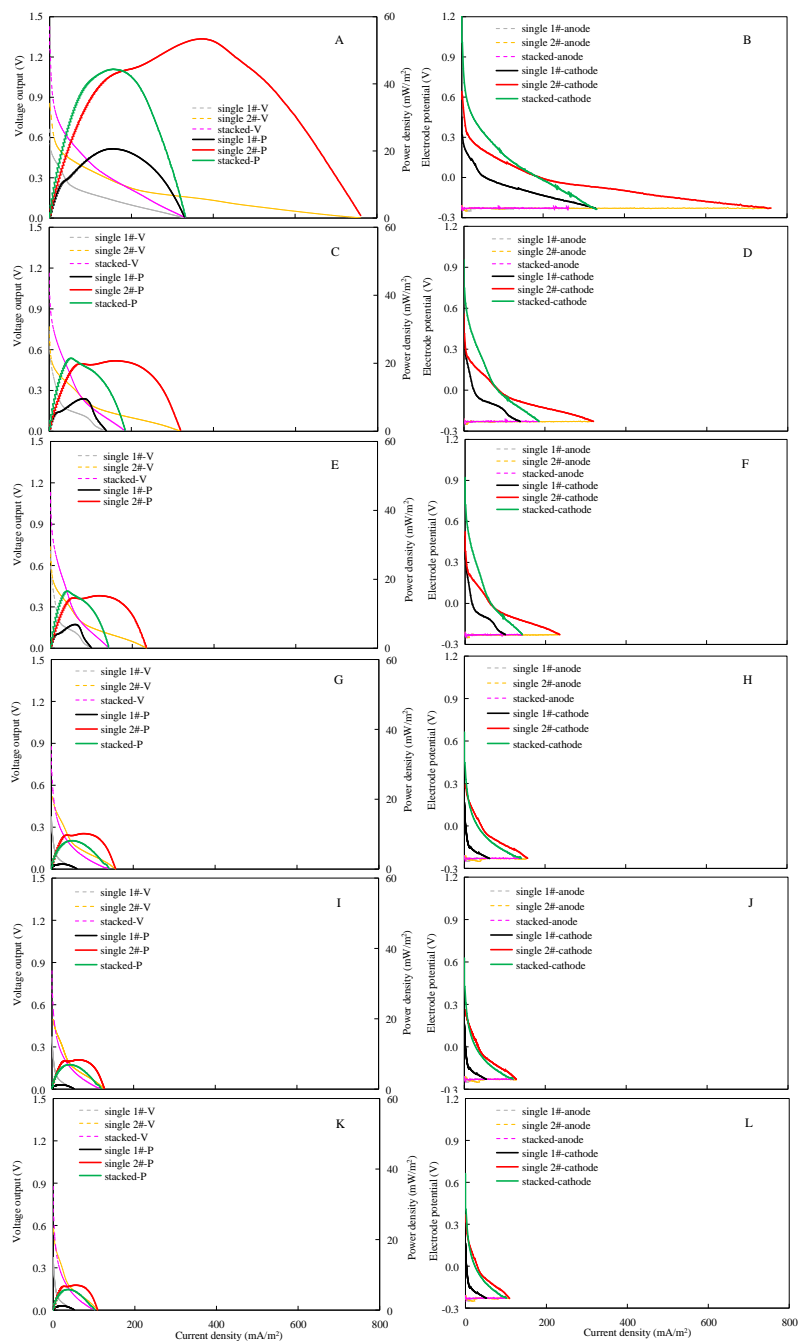


**Fig. S6** (A, C, E, G, I and K) Polarization curves and (B, D, F, H, J and L) electrode potentials of the stacked BESs at an initial pH of (A and B) 1.5, (C and D) 2.0, (E and F) 2.5, (G and H) 3.0, (I and J) 3.5, or (K and L) 4.0.

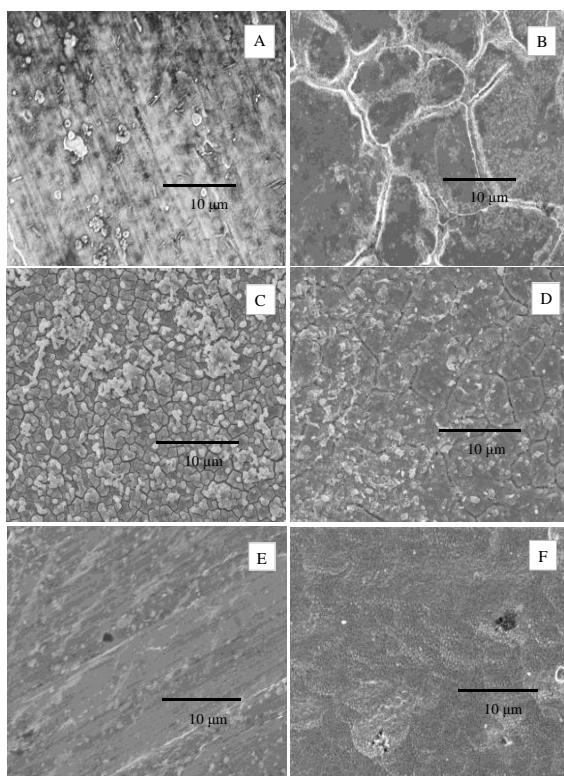


**Fig. S7** Morphology of W and Mo deposits on the cathodes of (A, C and E) the 1# and (B, D and F) the 2# units in the stacked BESs at an initial pH of (A and B) 1.5, (C and D) 2.0 or (E and F) 4.0 (W/Mo molar ratio = 1: 1).

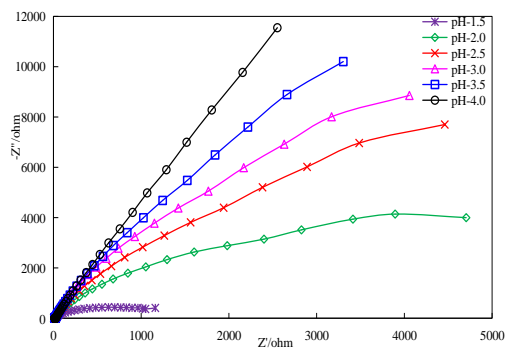


**Fig. S8** EIS analysis at various initial pHs (W/Mo molar ratio = 1 : 1, cathode: SSS in the 1# and CR in the 2# units).





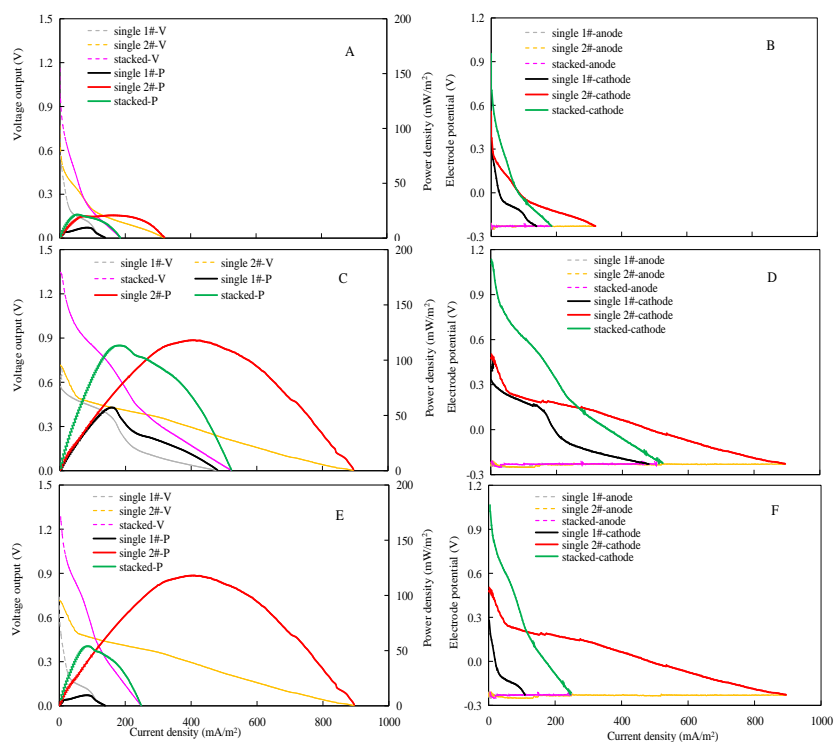


**Fig. S9** (A, C and E) Polarization curves and (B, D and F) electrode potentials of the stacked BESs with cathode materials of (A and B) same SSS, (C and D) same CR and (E and F) CR in the 2# unit and SSS in the 1# units (W/Mo molar ratio = 1 : 1; initial pH = 2.0).

**Table S1** Molybdenum and tungsten binding energies and corresponding area percent of deposits on cathodes of the 1# and the 2# units in the stacked BESs at various initial pHs or W/Mo molar ratios

Condition		Mo3d <sub>3/2</sub> (eV)			Mo3d <sub>5/2</sub> (eV)			W4f <sub>5/2</sub> (eV)	W4f <sub>7/2</sub> (eV)	Mo (%)			W (%)
		Mo <sup>4+</sup>	Mo <sup>5+</sup>	Mo <sup>6+</sup>	Mo <sup>4+</sup>	Mo <sup>5+</sup>	Mo <sup>6+</sup>	W <sup>6+</sup>	W <sup>6+</sup>	Mo <sup>4+</sup>	Mo <sup>5+</sup>	Mo <sup>6+</sup>	W <sup>6+</sup>
Initial	1#	233.2	234.5	235.7	230.1	231.4	232.6	37.6	35.4	48	33	19	100
pH 1.5	2#	233.1	234.4	236.0	230.0	231.3	232.9	37.9	35.8	26	41	33	100
Initial	1#	233.1	234.1	235.7	230.0	231.1	232.9	37.9	35.8	13	38	49	100
pH 4.0	2#	233.2	234.5	235.7	230.0	231.0	232.6	37.7	35.6	8	36	56	100
W : Mo =	1#	233.1	234.4	236.0	230.0	231.3	232.9	37.9	35.8	33	45	22	100
0.01 : 1	2#	233.2	234.2	235.7	230.1	230.8	232.2	37.6	35.4	18	38	44	100
W : Mo =	1#	233.1	234.2	236.0	230.0	231.1	232.9	37.7	35.6	12	32	56	100
1 : 0.01	2#	233.2	234.1	235.7	230.1	231.0	232.6	37.6	35.4	4	45	51	100

**Table S2** Component analysis of internal resistance of catholyte at various W/Mo molar ratios, and initial pHs.

W : Mo	R <sub>o</sub>	R <sub>p</sub>	R <sub>d</sub>	initial pH	R <sub>o</sub>	R <sub>p</sub>	R <sub>d</sub>
1 : 0.05	16.3	37.7	12810	1.5	6.9	10.1	456
1 : 0.1	14.8	25.7	11500	2.0	11.8	24.9	6744
1 : 1	11.8	24.9	6744	2.5	13.1	30.2	7967
0.1 : 1	10.7	16.6	1548	3.0	13.6	34.9	8976
0.05 : 1	10.1	28.6	2552	3.5	14.9	98.8	10987
0.01 : 1	10.4	37.3	4702	4.0	17.8	121.1	11987
Single W	17.4	134.5	14320				
Single Mo	16.5	64.4	6385				

1 *March 21, 2018*

2  
3 *Submitted to J Hazard Mater*

4  
5  
6 **Deposition and separation of W and Mo from aqueous solutions with**  
7  
8  
9 **simultaneous hydrogen production in stacked bioelectrochemical**  
10  
11 **systems (BESs): Impact of heavy metals W(VI)/Mo(VI) molar ratio,**  
12  
13 **initial pH and electrode material**  
14  
15  
16

17  
18  
19  
20 Liping Huang<sup>1,\*</sup>, Ming Li<sup>1</sup>, Yuzhen Pan<sup>2</sup>, Xie Quan<sup>1</sup>, Jinhui Yang<sup>2</sup>, Gianluca Li Puma<sup>3,\*</sup>  
21  
22  
23  
24

25  
26 1. Key Laboratory of Industrial Ecology and Environmental Engineering, Ministry of  
27  
28 Education (MOE), School of Environmental Science and Technology, Dalian University of  
29  
30 Technology, Dalian 116024, China  
31

32  
33 2. College of Chemistry, Dalian University of Technology, Dalian 116024, China  
34  
35

36  
37 3. Environmental Nanocatalysis & Photoreaction Engineering, Department of Chemical  
38  
39 Engineering, Loughborough University, Loughborough LE11 3TU, United Kingdom  
40  
41  
42  
43  
44  
45  
46

47 **Corresponding authors:**

48  
49  
50 (L. Huang) [lipinghuang@dlut.edu.cn](mailto:lipinghuang@dlut.edu.cn)  
51

52  
53 (G. Li Puma) [g.lipuma@lboro.ac.uk](mailto:g.lipuma@lboro.ac.uk)  
54  
55  
56  
57

58 The authors declare no competing financial interest.  
59  
60  
61

1           **Abstract:** The deposition and separation of W and Mo from aqueous solutions  
2  
3 with simultaneous hydrogen production was investigated in stacked  
4  
5 bioelectrochemical systems (BESs) composed of microbial electrolysis cell (1#)  
6  
7 serially connected with parallel connected microbial fuel cell (2#). The impact of  
8  
9 W/Mo molar ratio (in the range 0.01 mM : 1 mM and vice-versa), initial pH (1.5 to  
10  
11 4.0) and cathode material (stainless steel mesh (SSM), carbon rod (CR) and titanium  
12  
13 sheet (TS)) on the BES performance was systematically investigated. The  
14  
15 concentration of Mo(VI) was more influential than W(VI) in determining the rate of  
16  
17 deposition of both metals and the rate of hydrogen production. Complete metal  
18  
19 recovery was achieved at equimolar W/Mo ratio of 0.05 mM : 0.05 mM. The rates of  
20  
21 metal deposition and hydrogen production increased at acidic pH, with the fastest  
22  
23 rates at pH 1.5. The morphology of the metal deposits and the valence of the Mo were  
24  
25 correlated with W/Mo ratio and pH. CR cathodes (2#) coupled with SSM cathodes  
26  
27 (1#) achieved a significant rate of hydrogen production ( $0.82 \pm 0.04 \text{ m}^3/\text{m}^3/\text{d}$ ) with W  
28  
29 and Mo deposition ( $0.049 \pm 0.003 \text{ mmol/L/h}$  and  $0.140 \pm 0.004 \text{ mmol/L/h}$  (1#);  $0.025$   
30  
31  $\pm 0.001 \text{ mmol/L/h}$  and  $0.090 \pm 0.006 \text{ mmol/L/h}$  (2#)).  
32  
33  
34  
35  
36  
37  
38  
39  
40  
41  
42  
43  
44  
45  
46

47           **Keywords:** Bioelectrochemical system; microbial fuel cell; microbial electrolysis  
48  
49 cells; W and Mo deposition; hydrogen production  
50  
51  
52  
53  
54  
55  
56  
57  
58  
59  
60  
61  
62  
63  
64  
65

## 1 Introduction

Tungsten (W) and molybdenum (Mo) transition metals are valuable alloying resources used in various products such as electrochromic materials, gas sensors and lithium ion batteries, in addition to be contained in a range of materials such as special steels and catalysts for petrochemical industries [1-2]. The 2011 annual global production of W and Mo has been reported as 73000 t and 264000 t respectively, with over 80% of W and nearly 40% of Mo being produced in China [3-4]. The extraction of W and Mo from natural ores is an energy intensive process, requiring approximately 11600 kWh/ton of products [5]. The ore dressing wastewater produced during the extraction process of the metals contains a large amount of W and Mo ranging from 10 mg/L to 1000 mg/L, in addition to their existence in the leaching liquor of the spent industrial products [3,6]. The environmental and economic sustainability of the mining process, therefore, requires the recovery and separation of W and Mo from the leaching liquor and from industrial wastewater.

Conventional processes that have been proposed for the extraction and recovery of W and Mo from mining ores include solvent extraction, ion exchange, membrane separation, chemical precipitation and electrochemical treatment [3,7-9]. However, significant challenges remain, including the reduction of the energy consumption and the treatment cost, the reduction of the sludge produced during the treatment and the requirement of bringing the concentration levels of W(VI) and Mo(VI) in the wastewater effluents below the required environmental standards.

This study addresses novel bioelectrochemical systems (BESs) which may

1 provide an alternative and innovative method for the simultaneous recovery and  
2  
3 separation of W and Mo from industrial and mining aqueous effluents [10]. BES  
4  
5 multifunctional metallurgical processes have been conceived and intensively  
6  
7 investigated, in recent years since they provides cost-effective methods for the  
8  
9 extraction and separation of metals [11-12]. In BESs organic matter is oxidized in the  
10  
11 anodic chamber while dissolved metals may be simultaneously either reduced in the  
12  
13 cathodic chamber or oxidized in the anodic chamber, with the potential of producing  
14  
15 free energy [11-14]. BESs operate with zero or minimal external energy consumption,  
16  
17 generate very little sludge and require minimal reactor maintenance [15-18]. Multiple  
18  
19 metals including V(V), Cr(VI), As(III), Tl (I), Cd(II), Mn(II), Co(II), Ni(II) and Cu(II)  
20  
21 [11-12,16,19-27] have been recovered in single units of either microbial fuel cell  
22  
23 (MFC) or microbial electrolysis cell (MEC). Differently, stacked metallurgical BESs,  
24  
25 configured with MFC units providing in-situ the voltage output to drive the operation  
26  
27 of electrically connected MECs, exhibited more merits than single MFC or MEC units.  
28  
29 Stacked metallurgical BESs have been conceptually explored for the recovering and  
30  
31 separation of multiple metals such as, Cr(VI), Cu(II) and Cd(II), Cu(II) and Co(II),  
32  
33 and Cu(II), Co(II) and Li(I) [28-32]. The concept of using optimized MFC and MEC  
34  
35 stacked BESs for the efficient deposition and separation of W(VI) and Mo(VI) from  
36  
37 mixed aqueous solutions with simultaneous hydrogen production has been  
38  
39 demonstrated in our recent study [10] using an initial pH of 2.0, a W(VI)/Mo(VI)  
40  
41 molar ratio of 1 : 1 and a stainless steel sheet cathode electrode. However, the impact  
42  
43 of the operating parameters require further investigation, in order to optimize the  
44  
45  
46  
47  
48  
49  
50  
51  
52  
53  
54  
55  
56  
57  
58  
59  
60  
61  
62  
63  
64  
65



1 deposition, separation and recovery of W and Mo metals from practical wastes and  
2  
3 wastewaters, with simultaneous hydrogen production.  
4  
5

6 The concentrations of W(VI) and Mo(VI) in the ores and leaching liquor of spent  
7  
8 catalysts are dependent on the characteristics of the mining site or industrial process,  
9  
10 with some cases presenting an excess of Mo(VI) and lower amount of W(VI) or  
11  
12 vice-versa [4-6,9]. The concentrations of W(VI) and Mo(VI) in the ore dressing  
13  
14 wastewater produced during the extraction process, are also closely correlated with  
15  
16 the extraction process used. Thus, significant fluctuations in the concentrations of  
17  
18 W(VI) and Mo(VI) in the wastewater generally occurs [3,5-6], which translates in  
19  
20 variable rates of W and Mo deposition, and thus variable rates of hydrogen production  
21  
22 in the MEC units of the stacked BESs. Similarly, pH plays a significant role on the  
23  
24 nature of the W and Mo ionic forms present in aqueous solution, on the degree of  
25  
26 polymerization of W in electrochemical processes [33], and on the rate of hydrogen  
27  
28 evolution in MECs [34-35]. Furthermore, the cathode material also plays an important  
29  
30 role. A range of cathodes materials including carbon rod, carbon plate, stainless steel  
31  
32 mesh and titanium sheet have been proposed for the recovery of Co(II), Cu(II) and/or  
33  
34 Cd(II) in single MFC or MEC units and even stacked BESs [29-31,36-39]. However,  
35  
36 the performance of only a few of them has been compared under the same operational  
37  
38 conditions [30]. The materials used to recover W and Mo in conventional  
39  
40 electrochemical processes operated under galvanic mode include titanium, platinum,  
41  
42 nickel, copper and gold [2,40-41]. In particular, W and Mo deposits on these materials  
43  
44 also may act as catalysts for the evolution of hydrogen [40-42]. Therefore, the  
45  
46  
47  
48  
49  
50  
51  
52  
53  
54  
55  
56  
57  
58  
59  
60  
61  
62

1 reduction of heavy metals and the reduction of protons to hydrogen may be competing  
2  
3 processes for the cathodic electrons, particularly at low metal concentrations  
4  
5  
6 [37-38,43]. Such occurrence may call for the use of different cathodic material and/or  
7  
8  
9 experimental conditions depending on the desired treatment objectives.

10  
11 In this study, stacked BESs were constructed to investigate the impact of the  
12  
13 W(VI)/Mo(VI) molar ratio (herein reported as W/Mo for brevity), the initial pH and  
14  
15 the cathode electrode material on the rates of W and Mo deposition from aqueous  
16  
17 solutions, and on the simultaneous rates of hydrogen production. The W and Mo  
18  
19 molar ratio was varied in the range of 0.01 : 1 and vice-versa. The initial pH in the  
20  
21 cathodic chamber containing the mixed metals ranged from 1.5 to 4.0, and stainless  
22  
23 steel mesh (SSM), carbon rod (CR) and titanium sheet (TS) were systematically  
24  
25 explored as cathode materials. The BESs system performance was elucidated by  
26  
27 linear sweep voltammetry (LSV), scanning electronic microscopy (SEM), X-ray  
28  
29 photoelectron spectroscopy (XPS) and electrochemical impedance spectroscopy (EIS).  
30  
31 Cathode potential, current and voltage output from the MFC units applied to the  
32  
33 MECs (applied voltage) were employed to assess the rate of W and Mo deposition,  
34  
35 the metals separation factor and the rate of hydrogen production. The concept of  
36  
37 complete metal recovery was also investigated.  
38  
39  
40  
41  
42  
43  
44  
45  
46  
47  
48

## 49 **2 Materials and Methods**

### 50 *2.1 BESs assembly*

51  
52 Stacked BESs were designed with one MFC (1#) serially connected with three  
53  
54 parallel MFCs (2#) (Fig. S1) as a result of previous optimization of the modules with  
55  
56  
57  
58  
59  
60  
61  
62  
63  
64  
65

1 multiple units [10]. Each reactor unit was made of two-chambers (14 ml operating  
2  
3 volume) separated by a cation exchange membrane (CMI-7000 Membranes  
4  
5 International, Glen Rock, NJ). Porous graphite felts ( $1.0 \times 1.0 \times 1.0$  cm, San Ye Co.,  
6  
7 Beijing, China) were used as anodes [44], whereas SSS ( $2.0 \times 2.0$  cm, Qing Yuan Co.,  
8  
9 China) were used as the cathodes of both the 1# and the 2# units. A glass tube with an  
10  
11 inner diameter of 8 mm was glued to the top of the 1# unit to create a total headspace  
12  
13 of 12 mL for hydrogen collection [10,44]. A reference electrode (Ag/AgCl, 195 mV vs.  
14  
15 SHE) was installed in the cathodic chamber to measure the electrode potential, with  
16  
17 all potentials reported vs. SHE. The reactors were wrapped with aluminum foil to  
18  
19 ensure darkness, to avoid the algae growth on the anodes and possible side reactions  
20  
21 on the cathodes. The properties of the 2# units have been reported as average values  
22  
23 for the sake of clarity, since the differences among the three units connected in  
24  
25 parallel were insignificant.  
26  
27  
28  
29  
30  
31  
32  
33  
34  
35

## 36 *2.2 Inoculation and operation*

37  
38

39 Anodic inoculation was exactly the same as previously described [28-30]. Mixed  
40  
41 W(VI) and Mo(VI) aqueous solutions were prepared using  $\text{Na}_2\text{WO}_4 \cdot 2\text{H}_2\text{O}$  and  
42  
43  $\text{Na}_2\text{MoO}_4 \cdot 2\text{H}_2\text{O}$  (Kaida Chemical Co. Ltd., Tianjin, China). The W and Mo molar  
44  
45 ratio (mM : mM) in the cathodic chamber was varied as 1 : 1, 0.1 : 1, 0.05 : 1, 0.01 :  
46  
47 1, 1 : 0.1, 1 : 0.05, and 1 : 0.01, and the initial pH was 1.5, 2.0, 2.5, 3.0, 3.5 and 4.0.  
48  
49 Also experiments were conducted at equimolar concentrations of 0.1 : 0.1 and 0.05 :  
50  
51 0.05. Solution conductivity was invariably regulated to the maximal 6.60 mS/cm  
52  
53 associated with the most acidic pH of 1.5, to exclude the effect of solution  
54  
55  
56  
57  
58  
59  
60  
61  
62  
63  
64  
65

1 conductivity on system performance [45]. SSM, CR (Chijiu Duratight Carbon Co.,  
2 Qingdao, China) or TS (Qingyuan Co., China) cathodes (1#) were coupled with  
3 SSM or CR cathodes (2#) with equal geometric areas ( $2.0 \times 2.0$  cm). The stacked  
4 BESs were operated in fed-batch mode at room temperature ( $25 \pm 3$  °C). Three  
5 duplicate BESs were used in all experiments.  
6  
7  
8  
9  
10  
11  
12

13  
14 Control experiments with single W(VI) or Mo(VI) metal in solution were  
15 performed to reflect the impact of the binary-component on the system performance.  
16  
17 Control experiments under open circuit conditions (OCCs) reflected the effect of  
18 current on W and Mo deposition. Other control experiments using the 1# or the 2#  
19 units only were performed to illustrate the roles played by each unit on system  
20 performance.  
21  
22  
23  
24  
25  
26  
27  
28  
29

### 30 *2.3 Measurements and analyses*

31  
32 The W(VI) and Mo(VI) concentrations in the catholyte were measured using  
33 standard methods [46]. The electrical data were monitored with an automatic data  
34 acquisition system (PISO-813, Hongge Co.,Taiwan). The electrical current was  
35 calculated from the voltage read across a small external resistance ( $10 \Omega$ ). The  
36 hydrogen in the headspace of the cathodic chambers was sampled and analyzed as  
37 previously described [10,37-38,44].  
38  
39  
40  
41  
42  
43  
44  
45  
46  
47  
48

49  
50 The rates of W ( $R_W$ , mmol/L/h) and Mo ( $R_{Mo}$ , mmol/L/h) deposition on the  
51 cathodes was calculated from Eqs. S1 – 2, whereas the power density was normalized  
52 to the projected surface area of the separator [10]. The rate of hydrogen production  
53 and the separation factor  $\varepsilon$  were calculated from Eqs. S3 and S4, respectively [10,36].  
54  
55  
56  
57  
58  
59  
60  
61

1 LSVs were conducted using a potentiostat (CHI 770c, Chenhua, Shanghai) at a scan  
2  
3 rate of 1.0 mV/s. The inner resistance of the BES units at different initial pH and  
4  
5 W/Mo molar ratios was quantified by EIS (Bio-Logic VMP3) as previously described  
6  
7 [10,39,43,47]. The morphologies and valences of the products on the cathode were  
8  
9 observed by SEM (Hitachi S-4800) and determined by XPS (Kratos AXIS Ultra  
10  
11 DLD). One-way ANOVA in SPSS 19.0 was used to analyze the differences among the  
12  
13 data, and all of the data indicated significance levels of  $p < 0.05$ .  
14  
15  
16  
17  
18  
19

### 20 **3 Results and discussion**

#### 21 *3.1 The impact of W/ Mo molar ratio*

22  
23  
24  
25 At a fixed Mo concentration of 1.0 mM, higher W concentrations favored the  
26  
27 deposition of W (Fig. 1A) and negligibly affected the deposition of Mo (Fig. 1B) in  
28  
29 both the 1# and the 2# units. The rate of deposition of W was  $0.079 \pm 0.003$  mmol/L/h  
30  
31 (1#) and  $0.050 \pm 0.001$  mmol/L/h (2#) (Fig. 1A), while for Mo it was  $0.193 \pm 0.002$   
32  
33 mmol/L/h (1#) and  $0.138 \pm 0.001$  mmol/L/h (2#) (Fig. 1B), at the higher  
34  
35 concentration of W investigated (1.0 mM). Greater amounts of W and Mo were  
36  
37 invariably deposited in the 1# unit, rather than in the 2# units (Fig. 1A and B), which  
38  
39 was ascribed to the voltage output from the 2# units and applied to the 1# unit (Fig.  
40  
41 1C) for the consequent higher currents (Fig. 1D) and more negative cathode potentials  
42  
43 (Fig. 1E) in the 1# unit. Higher current and more negative potentials favor the rate of  
44  
45 deposition of oxidative metals on the cathodes of BESs [11-12]. The observed  
46  
47 polarization curves and electrode potentials as a function of the current (Fig. S2)  
48  
49 further demonstrated the significance and impact of the W concentration on the BESs  
50  
51  
52  
53  
54  
55  
56  
57  
58  
59  
60  
61  
62  
63  
64  
65

1 performance. The similar values of applied voltages, in the range 0.10 – 0.11 V (Fig.  
2  
3 1C), led to the simultaneous evolution of hydrogen at variable rates (0.34 – 0.41  
4  
5 m<sup>3</sup>/m<sup>3</sup> d) in the 1# unit, during the deposition of the metals (Fig. 1F). This result also  
6  
7 reflected an insignificant effect of W concentrations on the rate of hydrogen  
8  
9 production in the 1# unit.  
10  
11  
12

### 13 Here Fig. 1

14  
15  
16 At a fixed W concentration of 1.0 mM, a decrease in Mo concentration decreased  
17  
18 the rate of deposition of W (Fig. 2A) and Mo (Fig. 2B) in both the 1# and the 2# units  
19  
20 with varying degrees. This resulted in high values of the separation factors equal to  
21  
22 717 ± 4 (1#) and 200 ± 8 (2#), at a W/Mo molar ratio of 1 : 0.1 (Table 1), which were  
23  
24 significantly higher than the values (80 to 105) reported in conventional solvent  
25  
26 extraction processes [8]. Lower Mo concentrations led to decreased currents (Fig. 2C)  
27  
28 and less negative cathode potentials (Fig. 2D) in the 1# unit. It also significantly  
29  
30 decreased the applied voltages (Fig. 2E), consistent with the polarization curves and  
31  
32 the cathodic potentials as a function of current (Fig. S3), all of which explained the  
33  
34 decreased rate of hydrogen production observed (Fig. 2F).  
35  
36  
37  
38  
39  
40  
41  
42  
43

44 Collectively, the results in Fig. 1 and Fig. 2 show that Mo(VI) was more  
45  
46 influential than W(VI) in determining an increase in the rate of deposition of both  
47  
48 metals and in the rate of hydrogen production. The influential role of Mo(VI) for  
49  
50 either W(VI) recovery or as catalysts for hydrogen evolution in conventional  
51  
52 chemical/electrochemical processes has been also shown in other studies [2,7-8,41,48].  
53  
54  
55  
56  
57

58 Binary mixtures of W(VI) and Mo(VI) reportedly forms diverse molybdotungstates  
59  
60  
61

1 species, which favor the further deposition of W(VI), however, the deposition of W is  
2  
3 inhibited in the absence of Mo(VI) in conventional chemical/electrochemical  
4  
5 processes [7,49]. Thus, at high W/Mo molar ratios, the rates of deposition of the  
6  
7 metals and hydrogen production were diminished in the stacked BESs.  
8  
9

10  
11  
12 **Here Fig. 2**

13  
14 **Here Table 1**

15  
16  
17 The W/Mo molar ratio also influenced the morphology of the metals deposited  
18  
19 over the stacked BESs cathodes. Smaller and more homogeneous particles were  
20  
21 observed on the cathodes of both the 1# (Fig. S4A) and the 2# (Fig. S4B) units at a  
22  
23 W/Mo molar ratio of 1 : 0.01, in comparison to those at a W/Mo ratio of 1 : 1 (Fig.  
24  
25 S4C and D). Conversely, a W/Mo molar ratio of 0.01 : 1 led to the presence of  
26  
27 irregular deposits in the 1# unit (Fig. S4E) complemented by dense layer deposits in  
28  
29 the 2# units (Fig. S4F).  
30  
31  
32  
33  
34  
35

36  
37 The XPS spectra for the W4f or Mo3d core electronic transitions exhibited the  
38  
39 characteristic 4f<sub>7/2</sub> and 4f<sub>5/2</sub> or 3d<sub>5/2</sub> and 3d<sub>3/2</sub> doublet of peaks at 35.8 and 37.9 eV  
40  
41 assigned to W(VI) in WO<sub>3</sub> [50], whereas the peaks at 232.9 and 236.0, 231.4 and  
42  
43 234.5, and 230.0 and 233.1 eV corresponded to Mo3d<sub>5/2</sub> and Mo3d<sub>3/2</sub> in MoO<sub>3</sub>,  
44  
45 Mo<sub>2</sub>O<sub>5</sub> and MoO<sub>2</sub>, respectively (Table S1) [42]. Similar peaks at 35.9 and 38.1 eV  
46  
47 were observed in both the 1# (Fig. 3A and E) and the 2# (Fig. 3C and G) units  
48  
49 regardless of the W/Mo molar ratio (i.e., high (1 : 0.01) (Fig. 3A and C) or low (0.01 :  
50  
51 1) (Fig. 3E and G)). The catholyte at the end of each fed-batch cycle operation  
52  
53 instantly changed in color in the absence of N<sub>2</sub> protection, consistent with the report  
54  
55  
56  
57  
58  
59  
60  
61  
62  
63  
64  
65

1 that W(V) as a reduced product is highly unstable and easily oxidized to W(VI) due to  
2  
3 the sampling procedures [2]. Thus, these similar peaks (Fig. 3A, 3C, 3E and 3G)  
4  
5 could presumably be the result from the re-oxidation of the W reduced products. In  
6  
7 contrast, the valence of the Mo deposits was strongly correlated with the W/Mo molar  
8  
9 ratio and varied among the different units (Fig. 3B, D, F and H). Stronger Mo(V) and  
10  
11 Mo(IV) signals were observed at a low W/Mo molar ratio of 0.01 : 1 in the 1# unit  
12  
13 (Fig. 3F) rather than in the 2# units (Fig. 3H and Table S1), while much weaker  
14  
15 signals were observed at a W/Mo molar ratio of 1 : 0.01 in the 1# unit (Fig. 3B and  
16  
17 Table S1). This result demonstrates that Mo(VI) was more easily reduced to Mo(V)  
18  
19 rather than Mo(IV).  
20  
21  
22  
23  
24  
25  
26

### 27 Here Fig. 3

28  
29 The variation of the cathode resistances at different W/Mo molar ratios was  
30  
31 determined by EIS (Fig. 4) through the fitting of the observed spectra to equivalent  
32  
33 electrical circuits (Fig. S5 and Table S2). The ohmic resistance ( $R_o$ ) at low W/Mo  
34  
35 ratios of 0.05 : 1 and 0.01 : 1 was equivalent to that at equimolar W/Mo ratio of 1 : 1,  
36  
37 but the polarization resistance ( $R_p$ ) was higher and the diffusional resistance ( $R_d$ ) was  
38  
39 lower (Fig. 4A and Table S2). Therefore, the deposition of Mo increased the activation  
40  
41 loss and decreased the diffusional loss. High W/Mo ratios instead, invariably  
42  
43 increased the resistances  $R_o$ ,  $R_p$  and  $R_d$  (Fig. 4B and Table S2), consistent with the  
44  
45 polarization curves and cathode potentials as a function of current (Fig. S3), implying  
46  
47 that the W deposits had a stronger effect than Mo on the resistances. In the control  
48  
49 experiments performed with either W(VI) or Mo(VI) in solution, the resistances  $R_o$ ,  
50  
51  $R_p$  and  $R_d$  were appreciably higher than those observed with the binary metals (Fig.  
52  
53  
54  
55  
56  
57  
58  
59  
60  
61  
62  
63  
64  
65



1 4C and Table S2).

2  
3 **Here Fig. 4**

4  
5  
6 *3.2 Effect of initial pH*

7  
8  
9 The initial pH of the catholyte was varied in the range from 1.5 to 4.0. At acidic  
10 pH of 1.5 and 2.0 the highest rates of W and Mo deposition were observed, equaling  
11  
12  $0.0785 \pm 0.003 - 0.0808 \pm 0.004$  mmol/L/h (W) and  $0.190 \pm 0.004 - 0.193 \pm 0.002$   
13  
14 mmol/L/h (Mo) in the 1# unit, and  $0.0501 \pm 0.001 - 0.0548 \pm 0.001$  mmol/L/h (W)  
15  
16 and  $0.138 \pm 0.001 - 0.144 \pm 0.005$  mmol/L/h (Mo) in the 2# units (Fig. 5A and B).  
17  
18 Higher amounts of metals deposited in the 1# than in the 2# units, were generally  
19  
20 accompanied by higher separation factors in the former (Table 1), consistent with the  
21  
22 higher currents (Fig. 5C) and the more negative cathode potentials (Fig. 5D) observed  
23  
24 in the 1# unit, both of which generally favor the reduction of oxidative substrates  
25  
26 [11,51]. A decreasing trend of the rate of metal deposition was observed at an initial  
27  
28 pH higher than 2.0.  
29  
30  
31  
32  
33  
34  
35  
36  
37  
38

39 Smaller polarization loss (Fig. S6), higher applied voltage (Fig. 5E) and an  
40  
41 appreciable higher rate of hydrogen production (Fig. 5F) were observed at more  
42  
43 acidic initial pH in the 1# unit, consistent with the decrease of the pH in the effluents  
44  
45 from  $5.93 \pm 0.08$  at an initial pH of 4.0 to  $2.27 \pm 0.06$  at pH 1.5. Other studies,  
46  
47 performed with MECs in the absence of W or/and Mo also reported faster rates of  
48  
49 hydrogen production at more acidic pH [34-35]. Considering the similar rates of W  
50  
51 and Mo depositions at pH 1.5 and 2.0 (Fig. 5A and B), the significantly higher  
52  
53 hydrogen production at pH 1.5 implied that hydrogen evolution outcompeted the  
54  
55  
56  
57  
58  
59  
60  
61  
62

1 deposition of the metals for the available cathodic electrons, alike the electron  
2  
3 competition between reductive dechlorination and denitrification [52].  
4  
5

6 An experiment with pH controlled at 1.5 during the entire operational period was  
7  
8 purposely investigated to determine its effect on the metal deposition. An appreciable  
9  
10 higher rate of hydrogen production of  $2.14 \pm 0.07 \text{ m}^3/\text{m}^3/\text{d}$ , and enhanced W and Mo  
11  
12 deposition rates (W:  $0.0965 \pm 0.005 \text{ mmol/L/h}$ ; Mo:  $0.227 \pm 0.005 \text{ mmol/L/h}$ ) in the  
13  
14 1# unit were observed, compared to the results obtained without pH control ( $1.21 \pm$   
15  
16  $0.03 \text{ m}^3/\text{m}^3/\text{d}$ ,  $0.081 \pm 0.004 \text{ mmol/L/h}$  (W) and  $0.190 \pm 0.004 \text{ mmol/L/h}$  (Mo)). In  
17  
18 concert, the results observed supported a significant dependence of the rate of W and  
19  
20 Mo deposition with simultaneous hydrogen production on the pH in the catholyte.  
21  
22  
23  
24  
25  
26  
27

### 28 Here Fig. 5

29  
30 The morphology of the W and Mo deposits was significantly influenced by the  
31  
32 initial pH in the catholyte. Wider cracks and larger areas surrounded by the cracks in  
33  
34 both the 1# and the 2# units (Fig. S7A and B) were observed at pH 1.5, in comparison  
35  
36 to the results at pH 2.0 and 4.0, consistent with the morphology of Mn, Mo and W  
37  
38 co-deposits in conventional electrochemical processes [33]. Larger W and Mo grain  
39  
40 sizes were consistently observed in the 1# (Fig. S7A, C and E) than in the 2# units  
41  
42 (Fig. S7B, D and F), and the grain size was inversely correlated with the increase in  
43  
44 the initial pH in the same units. The higher currents observed in the 1# than in the 2#  
45  
46 units at the same pH (Fig. 5C) resulted in wider cracks and smaller grains, consistent  
47  
48 with the tungsten morphology influenced by current in conventional electrochemical  
49  
50 processes [53].  
51  
52  
53  
54  
55  
56  
57  
58  
59  
60  
61

1 The XPS binding energies (Fig. 6) for Mo and W deposits as well as the  
2  
3 corresponding area percent (Table S1) showed that at an initial pH 1.5 appreciable  
4  
5 higher Mo(IV) products were achieved in the 1# unit (48%, Fig. 6B and Table S2)  
6  
7 than in the 2 units (26%, Fig. 6F and Table S2), both of which were higher than the  
8  
9 results at an initial pH of 4.0 (13% in 1#, Fig. 6D and 8% in 2#, Fig. 6H and Table S2).  
10  
11 These results clearly demonstrate the dependency of the valences of the Mo deposits  
12  
13 on the initial pH. Similarly, the peaks associated with W deposits in the 1# unit at pH  
14  
15 1.5 (Fig. 6A) were apparently higher than either in the 2# units at the same pH (Fig.  
16  
17 6E) or in the same 1# unit but at pH 4.0 (Fig. 6C). The lowest peaks were observed in  
18  
19 the 2# units at pH 4.0 (Fig. 6G). Collectively, these results demonstrated a significant  
20  
21 dependency of the rate of W and Mo deposition, and even the dependence of the  
22  
23 valence of the Mo deposits, on the initial pH of the catholyte, and on the units of the  
24  
25 stacked BESs.  
26  
27  
28  
29  
30  
31  
32  
33  
34

### 35 Here Fig. 6

36  
37  
38  
39 EIS spectra were used to identify the components of the internal resistances as a  
40  
41 function of the initial pH.  $R_d$ ,  $R_p$  and  $R_o$  in concert exhibited increase trends with an  
42  
43 increase in the initial pH, from 456  $\Omega$ , 10.1  $\Omega$  and 6.9  $\Omega$  at a pH of 1.5, to 11987  $\Omega$ ,  
44  
45 121.1  $\Omega$  and 17.8  $\Omega$  at pH 4.0 (Fig. S8 and Table S2). These results clearly illustrated  
46  
47 the favorable effect of acidic pH on decreasing the internal resistances of the stacked  
48  
49 BESs, consistent with the results shown in Fig. 5.  
50  
51  
52

### 53 3.3 Effect of electrode material

54  
55  
56  
57  
58 The use of inexpensive SSS cathodes in both the 1# and the 2# units achieved the  
59  
60  
61

1 highest rate of W (Fig. 7A) and Mo deposition (Fig. 7B) with lower rates of hydrogen  
2  
3 production (Fig. 7F) and more polarization loss (Fig. S9A and B), in comparison to  
4  
5 the other electrodes combinations tested (Fig. 7A, B and F, Fig. S9). SSS cathodes (1#)  
6  
7 coupled with the CR cathodes (2#) exhibited similar more negative cathode potentials  
8  
9 and higher currents as the configuration using TS (1# unit) and CR (2#) cathodes (Fig.  
10  
11 7C and D), resulting in higher applied voltages (Fig. 7E) and the subsequent  
12  
13 significant rate of hydrogen production of  $0.82 \pm 0.04 \text{ m}^3/\text{m}^3/\text{d}$  (Fig. 7F) with W and  
14  
15 Mo deposition (W:  $0.049 \pm 0.003 \text{ mmol/L/h}$  (1#),  $0.025 \pm 0.001 \text{ mmol/L/h}$  (2#); Mo:  
16  
17  $0.140 \pm 0.004 \text{ mmol/L/h}$  (1#),  $0.090 \pm 0.006 \text{ mmol/L/h}$  (2#)) (Fig. 7A and B).  
18  
19 Hydrogen evolution is well known to increase the pH in solution [34], which in  
20  
21 consequence penalizes the deposition of W and Mo [10], explaining reduced rates of  
22  
23 W and Mo deposition at much more negative cathode potentials and higher currents  
24  
25 (Fig. 7A – D). The results collectively show that SSS (1#) and CR (2 #) represent  
26  
27 well-matched electrodes for efficient W and Mo deposition in the stacked BESs.  
28  
29  
30  
31  
32  
33  
34  
35  
36  
37  
38

39 **Here Fig. 7**

### 40 *3.4 Complete metal recovery*

41  
42 The results reported have shown that the W(VI)/Mo(VI) molar ratio significantly  
43  
44 affected the rate of metals deposition, as well as, the rate of hydrogen production in  
45  
46 the stacked BESs. W(VI)/Mo(VI) molar ratios smaller or equal to 1 : 1 favoured the  
47  
48 deposition of more W and Mo in the 1# than the 2# units with a negligible effect on  
49  
50 the rate of hydrogen production (Fig. 1). In contrast, W(VI)/Mo(VI) molar ratios  
51  
52 larger than 1 : 1 resulted in similar rates of deposition of both metals in both the 1#  
53  
54  
55  
56  
57  
58  
59  
60  
61  
62

1 and the 2# units, and more than halved the rate of hydrogen production (Fig. 2).  
2  
3 Further experiments with equimolar W(VI)/Mo(VI) molar ratios and lower initial  
4 metals concentrations (1 : 1, 0.1 : 0.1 and 0.05 : 0.05) were performed at an initial pH  
5  
6 of 2.0 with cathodes of SSS (1#) and CR (2#) to clarify the role of equimolar heavy  
7  
8 metals concentration on system performance. The rates of W (Fig. 8A) and Mo (Fig.  
9  
10 8B) deposition decreased when reducing the concentrations of the metals from 1 : 1 to  
11  
12 0.05 : 0.05. At the lower metals concentrations of 0.05 : 0.05, complete heavy metals  
13  
14 deposition was achieved in the 1# unit and almost complete deposition ( $94.3 \pm 2.2\%$   
15  
16 (W) and  $98.4 \pm 0.8\%$  (Mo)) occurred in the 2# units. Simultaneously, lower separation  
17  
18 factors (Table 1), smaller currents (Fig. 8C), more positive cathode potentials (Fig.  
19  
20 8D), lower applied voltages (Fig. 8E) and smaller rates of hydrogen production (Fig.  
21  
22 8F) were observed in comparison to the 1 : 1 case. These results demonstrate the  
23  
24 feasibility of these stacked BESs for either complete deposition of W and Mo at this  
25  
26 lower equivalent W and Mo concentrations, or higher rates of hydrogen production at  
27  
28 higher equivalent W and Mo concentrations.  
29  
30  
31  
32  
33  
34  
35  
36  
37  
38  
39  
40  
41

### 42 Here Fig. 8

43  
44 The deposition of binary mixtures of W(VI) and Mo(VI) in stacked BESs have  
45  
46 shown synergistic effects on the recovery of the metals and the simultaneous  
47  
48 production of hydrogen [10]. However, the optimization of such BESs required  
49  
50 further analysis to account for the impact of fluctuations in the concentration of heavy  
51  
52 metals and pH in the wastewater [4-6]. Furthermore, the electrode materials exert a  
53  
54 significant impact on the rates of other metals deposition and hydrogen production in  
55  
56  
57  
58  
59  
60  
61  
62  
63  
64  
65

1 BESs [35,37-37,54]. The elucidation of such effects is required for further  
2  
3 optimization of BESs, which could ultimately lead to industrial application.  
4  
5

6 The present study has illustrated the dependency of rates of W and Mo  
7  
8 deposition, as well as, hydrogen production on the W/Mo molar ratio, initial pH and  
9  
10 electrode material. Mo(VI) was more influential than W(VI) in determining an  
11  
12 increase in the rates of deposition of both metals and hydrogen production. The merit  
13  
14 of completely depositing W and Mo at an initial equimolar W/Mo ratio of 0.05 : 0.05  
15  
16 gives an advantage of this technology over conventional methods such as ion  
17  
18 exchange, chemical precipitation or adsorption [5,9], particularly with low-strength W  
19  
20 and Mo wastewaters from either the mining industry processes or wastewater  
21  
22 effluents. Such lower concentrations of metals in high strength wastewater could be  
23  
24 achieved with the partial recirculation of the effluent back to the influent [55-56] to  
25  
26 dilute the feed stream to the stacked BESs to optimal values, achieving enhanced  
27  
28 metal deposition and even complete separation of W and Mo (Fig. 1,2 and 8, and  
29  
30 Table 1). Practical implementation will also depend on the long-term operation of this  
31  
32 system, as well as, the process economics of BESs relative to conventional treatment  
33  
34 processes [54]. Although the present economic values of W and Mo deposits are  
35  
36 relatively low, the added complexity in the stacked BESs will be paid off with  
37  
38 increasing the demand on sustainability and elevated product values due to the  
39  
40 depletion of W and Mo resources. The simultaneous production of hydrogen  
41  
42 by-product in the MEC units of the stacked BESs further offsets the cost of this  
43  
44 technology, although further pilot and full-scale investigations are necessary to  
45  
46  
47  
48  
49  
50  
51  
52  
53  
54  
55  
56  
57  
58  
59  
60  
61  
62  
63  
64  
65

1 evaluate the long-term operation and stability of the system over feeds with  
2  
3 fluctuating physico/chemical properties.  
4  
5

#### 6 **4 Conclusions**

7  
8  
9 Stacked BESs composed of MEC (1#) serially connected with parallel connected  
10  
11 MFC (2#) have been shown to be effective in W and Mo deposition and separation  
12  
13 with simultaneous hydrogen production. It revealed a dramatic effect of the W/Mo  
14  
15 molar ratio, initial pH, and cathode material on the rates observed. The concentration  
16  
17 of Mo(VI) was more influential than W(VI) in determining the rate of deposition of  
18  
19 both metals and the rate of hydrogen production. Complete metal recovery was  
20  
21 achieved at equimolar W/Mo ratio of 0.05 mM : 0.05 mM. Acidic pH favored both the  
22  
23 deposition of the metals and the rate of hydrogen production. The BESs comprising  
24  
25 CR cathodes (2#) coupled with SSS cathodes (1#) achieved optimal performance. The  
26  
27 BESs studied here may provide an alternative and innovative method for the recovery  
28  
29 and separation of W and Mo from industrial and mining aqueous effluents with  
30  
31 simultaneous hydrogen production.  
32  
33  
34  
35  
36  
37  
38  
39  
40  
41  
42  
43  
44

#### 45 **Acknowledgments**

46  
47 The authors are gratefully acknowledge financial support from the National  
48  
49 Natural Science Foundation of China (Nos. 51578104 and 21777017), and the  
50  
51 Programme of Introducing Talents of Discipline to Universities (B13012).  
52  
53  
54

#### 55 **References**

56  
57 [1] D. Merki, X. Hu, Recent developments of molybdenum and tungsten sulfides as  
58  
59 hydrogen evolution catalysts, *Energy Environ. Sci.* 4 (2011) 3878-3888,  
60  
61 <http://dx.doi.org/10.1039/C1EE01970H>.  
62  
63  
64  
65

- 1 [2] S. Sun, T. Bairachna, E.J. Podlaha, Induced codeposition behavior of  
2 electrodeposited NiMoW alloys, *J. Electrochem. Soc.* 160 (2013) D434-D440,  
3 <http://dx.doi.org/10.1149/2.014310jes>.
- 4 [3] T.A. Lasheen, M.E. El-Ahmady, H.B. Hassib, A.S. Helal, Molybdenum metallurgy  
5 review: Hydrometallurgical routes to recovery of molybdenum from ores and  
6 mineral raw materials, *Miner. Process. Extr. Metall. Rev.* 36 (2015)145-173,  
7 <http://dx.doi.org/10.1080/08827508.2013.868347>.
- 8 [4] T. Ogi, T. Makino, K. Okuyama, W.J. Stark, F. Iskandar, Selective biosorption and  
9 recovery of tungsten from an urban mine and feasibility evaluation, *Ind. Eng. Chem.*  
10 *Res.* 55 (2016) 2903-2910, <http://dx.doi.org/10.1021/acs.iecr.5b04843>.
- 11 [5] Z. Zhao, C. Cao, X. Chen, G. Huo, Separation of macro amounts of tungsten and  
12 molybdenum by selective precipitation, *Hydrometallurgy* 108 (2011) 229-232,  
13 <https://doi.org/10.1016/j.hydromet.2011.04.006>.
- 14 [6] R.R. Srivastava, N.K. Mittal, B. Padh, B. Ramachandra Reddy, Removal of  
15 tungsten and other impurities from spent HDS catalyst leach liquor by an  
16 adsorption route, *Hydrometallurgy* 127-128 (2012) 77-83,  
17 <https://doi.org/10.1016/j.hydromet.2012.07.004>.
- 18 [7] L. Kondrachova, P.H. Benjamin, G. Vijayaraghavan, R.D. Williams, K.J.  
19 Stevenson, Cathodic electrodeposition of mixed molybdenum tungsten oxides from  
20 peroxo-polymolybdotungstate solutions, *Langmuir* 22 (2006) 10490-10498,  
21 <https://doi.org/10.1021/la061299n>.
- 22 [8] W. Guan, G. Zhang, C. Gao, Solvent extraction separation of molybdenum and  
23 tungsten from ammonium solution by H<sub>2</sub>O<sub>2</sub>-complexation, *Hydrometallurgy*  
24 127-128 (2012) 84-90, <https://doi.org/10.1016/j.hydromet.2012.07.008>.
- 25 [9] G. Huo, C. Peng, Q. Song, X. Lu, Tungsten removal from molybdate solutions  
26 using ion exchange, *Hydrometallurgy* 147-148 (2014) 217-222,  
27 <https://doi.org/10.1016/j.hydromet.2014.05.015>.
- 28 [10] L. Huang, M. Li, Y. Pan, Y. Shi, X. Quan, G. Li Puma, Efficient W and Mo  
29 deposition and separation with simultaneous hydrogen production in stacked  
30 bioelectrochemical systems, *Chem. Eng. J.* 327 (2017) 584-596,  
31 <http://dx.doi.org/10.1016/j.cej.2017.06.149>.
- 32 [11] H. Wang, Z.J. Ren, Bioelectrochemical metal recovery from wastewater: a review,  
33 *Water Res.* 66 (2014) 219-232, <http://dx.doi.org/10.1016/j.waters.2014.08.013>.
- 34 [12] Y.V. Nancharaiyah, S.Venkata Mohan, P.N.L. Lens, Biological and  
35 bioelectrochemical recovery of critical and scarce metals, *Trends Biotechnol.* 34  
36 (2016) 137-155, <http://dx.doi.org/10.1016/j.tibtech.2015.11.003>.
- 37 [13] X. Yong, D. Gu, Y. Wu, Z. Yan, J. Zhou, X. Wu, P. Wei, H. Jia, T. Zheng, Y. Yong,  
38 Bio-electron-fenton (BEF) process driven by microbial fuel cells for triphenyltin  
39 chloride (TPTC) degradation, *J. Hazard. Mater.* 324 (2017) 178-183,  
40 <http://dx.doi.org/10.1016/j.jhazmat.2016.10.047>.
- 41 [14] Q. Zhao, H. Yu, W. Zhang, F.T. Kabutey, J. Jiang, Y. Zhang, K. Wang, J. Ding,  
42 Microbial fuel cell with high content solid wastes as substrates: a review, *Front.*  
43 *Environ. Sci. Eng.* 11 (2017) 13, <http://dx.doi.org/10.1007/s11783-017-0918-6>.
- 44 [15] O. Modin, X. Wang, X. Wu, S. Rauch, K.K. Fedje,



- 1 Bioelectrochemical recovery of Cu, Pb, Cd, and Zn from dilute solutions, J. Hazard.  
2 Mater. 235 (2012) 291-297, <http://dx.doi.org/10.1016/j.jhazmat.2012.07.058>.
- 3 [16] M. Peiravi, S.R. Mote, M.K. Mohanty, J. Liu, Bioelectrochemical treatment of  
4 acid mine drainage (AMD) from an abandoned coal mine under aerobic condition,  
5 J. Hazard. Mater. 333 (2017) 329-338,  
6 <http://dx.doi.org/10.1016/j.jhazmat.2017.03.045>.
- 7 [17] O. Modin, F. Aulenta, Three promising applications of microbial  
8 electrochemistry for the water sector, Environ. Sci.: Water Res. Technol. 3 (2017)  
9 391-402, <http://dx.doi.org/10.1039/C6EW00325G>
- 10 [18] M. Wang, Q. Tan, J.F. Chiang, J. Li, Recovery of rare and precious metals from  
11 urban mines-A review, Front. Environ. Sci. Eng. 11 (5) (2017) 1,  
12 <http://dx.doi.org/10.1007/s11783-017-0963-1>.
- 13 [19] B. Zhang, C. Feng, J. Ni, J. Zhang, W. Huang, Simultaneous reduction of  
14 vanadium (V) and chromium (VI) with enhanced energy recovery based on  
15 microbial fuel cell technology, J. Power Sources 204 (2012) 34-39,  
16 <http://dx.doi.org/10.1016/j.jpowsour.2012.01.013>.
- 17 [20] H. Luo, G. Liu, R. Zhang, Y. Bai, S. Fu, Y. Hou, Heavy metal recovery combined  
18 with H<sub>2</sub> production from artificial acid mine drainage using the microbial  
19 electrolysis cell, J. Hazard. Mater. 270 (2014) 153-159,  
20 <http://dx.doi.org/10.1016/j.jhazmat.2014.01.050>.
- 21 [21] N. Colantonio, Y. Kim, Cadmium (II) removal mechanisms in microbial  
22 electrolysis cells, J. Hazard. Mater. 311 (2016) 134-141,  
23 <http://dx.doi.org/10.1016/j.jhazmat.2016.02.062>.
- 24 [22] Y. Li, B. Zhang, M. Cheng, Y. Li, L. Hao, Spontaneous arsenic (III) oxidation  
25 with bioelectricity generation in single-chamber microbial fuel cells, J. Hazard.  
26 Mater. 306 (2016) 8-12, <http://dx.doi.org/10.1016/j.jhazmat.2015.12.003>.
- 27 [23] Y. Dong, J.F. Liu, M.R. Sui, Y.P. Qu, J.J. Ambuchi, H.M. Wang, Y.J. Feng, A  
28 combined microbial desalination cell and electro dialysis system for  
29 copper-containing wastewater treatment and high-salinity-water desalination, J.  
30 Hazard. Mater. 321 (2016) 307-315,  
31 <http://dx.doi.org/10.1016/j.jhazmat.2016.08.034>.
- 32 [24] D. Wu, L. Huang, X. Quan, G. Li Puma, Electricity generation and bivalent  
33 copper reduction as a function of operation time and cathode electrode material in  
34 microbial fuel cells, J. Power Sources 307 (2016) 705-714,  
35 <https://doi.org/10.1016/j.jpowsour.2016.01.022>.
- 36 [25] R. Qiu, B. Zhang, J. Li, Q. Lv, S. Wang, Q. Gu, Enhanced vanadium (V)  
37 reduction and bioelectricity generation in microbial fuel cells with biocathode, J.  
38 Power Sources 359 (2017) 379-383,  
39 <http://dx.doi.org/10.1016/j.jpowsour.2017.05.099>.
- 40 [26] G. Wang, B. Zhang, S. Li, M. Yang, C. Yin, Simultaneous microbial reduction of  
41 vanadium (V) and chromium (VI) by *Shewanella loihica* PV-4, Bioresour. Technol.  
42 227 (2017) 353-358, <http://dx.doi.org/10.1016/j.jpowsour.2017.05.099>.
- 43 [27] Z. Wang, B. Zhang, Y. Jiang, Y. Li, C. He, Spontaneous thallium (I) oxidation  
44 with electricity generation in single-chamber microbial fuel cells, Appl. Energy 209  
45  
46  
47  
48  
49  
50  
51  
52  
53  
54  
55  
56  
57  
58  
59  
60  
61  
62  
63  
64  
65

- (2018) 33-42, <http://dx.doi.org/10.1016/j.apenergy.2017.10.075>.
- [28] J. Shen, Y. Sun, L. Huang, J. Yang, Microbial electrolysis cells with biocathodes and driven by microbial fuel cells for simultaneous enhanced Co(II) and Cu(II) removal, *Front. Environ. Sci. Eng.* 9 (2015) 1084-1095, <http://dx.doi.org/10.1007/s11783-015-0805-y>.
- [29] Y. Zhang, L. Yu, D. Wu, L. Huang, P. Zhou, X. Quan, G. Chen, Dependency of simultaneous Cr(VI), Cu(II) and Cd(II) reduction on the cathodes of microbial electrolysis cells self-driven by microbial fuel cells, *J. Power Sources* 273 (2015) 1103-1113, <https://doi.org/10.1016/j.jpowsour.2014.09.126>.
- [30] D. Wu, Y. Pan, L. Huang, X. Quan, J. Yang, Comparison of Co(II) reduction on three different cathodes of microbial electrolysis cells driven by Cu(II)-reduced microbial fuel cells under various cathode volume conditions, *Chem. Eng. J.* 266 (2015) 121-132, <https://doi.org/10.1016/j.cej.2014.12.078>.
- [31] D. Wu, Y. Pan, L. Huang, P. Zhou, X. Quan, H. Chen, Complete separation of Cu(II), Co(II) and Li(I) using self-driven MFCs-MECs with stainless steel mesh cathodes under continuous flow conditions, *Sep. Purif. Technol.* 147 (2015) 114-124, <http://dx.doi.org/10.1016/j.seppur.2015.04.016>.
- [32] M. Li, Y. Pan, L. Huang, Y. Zhang, J. Yang, Continuous flow operation with appropriately adjusting composites in influent for recovery of Cr(VI), Cu(II) and Cd(II) in self-driven MFC-MEC system, *Environ. Technol.* 38 (2017) 615-628, <http://dx.doi.org/10.1080/09593330.2016.1205149>.
- [33] N.A. Abdel Ghany, S. Meguro, N. Kumagai, K. Asami, K. Hashimoto, Adodically deposited Mn-Mo-Fe oxide anodes for oxygen evolution in hot seawater electrolysis, *Mater. Trans.* 44 (2003) 2114-2123.
- [34] Y. Ruiz, J.A. Baeza, A. Guisasola, Enhanced performance of bioelectrochemical hydrogen production using a pH control strategy, *ChemSusChem* 8 (2015) 389-397, <http://dx.doi.org/10.1002/cssc.201403083>.
- [35] A. Kadier, M. Sahaid Kalil, P. Abdeshahian, K. Chandrasekhar, A. Mohamed, N. Farhana Azman, W. Logroño, Y. Simayi, A. Abdul Hamid, Recent advances and emerging challenges in microbial electrolysis cells (MECs) for microbial production of hydrogen and value-added chemicals, *Renew. Sust. Energ. Rev.* 61 (2016) 501-525, <https://doi.org/10.1016/j.rser.2016.04.017>.
- [36] L. Huang, B. Yao, D. Wu, X. Quan, Complete cobalt recovery from lithium cobalt oxide in self-driven microbial fuel cell-microbial electrolysis cell systems, *J. Power Sources* 259 (2014) 54-64, <https://doi.org/10.1016/j.jpowsour.2014.02.061>.
- [37] Q. Wang, L. Huang, H. Yu, X. Quan, Y. Li, G. Fan, L. Li, Assessment of five different cathode materials for Co(II) reduction with simultaneous hydrogen evolution in microbial electrolysis cells, *Inter. J. Hydrogen Energy* 40 (2015) 184-196, <https://doi.org/10.1016/j.ijhydene.2014.11.014>.
- [38] Q. Wang, L. Huang, Y. Pan, P. Zhou, X. Quan, B.E. Logan, H. Chen, Cooperative cathode electrode and in situ deposited copper for subsequent enhanced Cd(II) removal and hydrogen evolution in bioelectrochemical systems, *Bioresour. Technol.* 200 (2016) 565-571, <https://doi.org/10.1016/j.biortech.2015.10.084>.
- [39] Q. Wang, L. Huang, Y. Pan, X. Quan, G. Li Puma, Impact of Fe(III) as an

- 1 effective mediator for enhanced Cr(VI) reduction in microbial fuel cells: Reduction  
2 of diffusional resistances and cathode overpotentials, *J. Hazard. Mater.* 321 (2017)  
3 896-906, <http://dx.doi.org/10.1016/j.jhazmat.2016.10.011>.
- 4 [40] N. Tsyntsar, H. Cesiulis, M. Donten, J. Sort, E. Pellicer, E.J. Podlaha-Murphy,  
5 Modern trends in tungsten alloys electrodeposition with iron group metals, *Surface*  
6 *Eng. Appl. Electrochem.* 48 (2012) 491-520,  
7 <http://dx.doi.org/10.3103/S1068375512060038>.
- 8 [41] T.G. Kelly, S.T. Hunt, D.V. Esposito, J.G. Chen, Monolayer palladium supported  
9 on molybdenum and tungsten carbide substrates as low-cost hydrogen evolution  
10 reaction (HER) electrocatalysts, *Inter. J. Hydrogen Energy* 38 (2013) 5638-5644,  
11 <https://doi.org/10.1016/j.ijhydene.2013.02.116>.
- 12 [42] M. Zhang, D. Lu, G. Yan, J. Wu, J. Yang, Fabrication of Mo+N-codoped TiO<sub>2</sub>  
13 nanotube arrays by anodization and sputtering for visible light-induced  
14 photoelectrochemical and photocatalytic properties, *J. Nanomater.* 2013 (2013) 1-9,  
15 <http://dx.doi.org/10.1155/2013/648346>.
- 16 [43] Q. Wang, L. Huang, X. Quan, Q. Zhao, Preferable utilization of in-situ produced  
17 H<sub>2</sub>O<sub>2</sub> rather than externally added for efficient deposition of tungsten and  
18 molybdenum in microbial fuel cells, *Electrochim. Acta* 247C (2017) 880-890,  
19 <https://doi.org/10.1016/j.electacta.2017.07.079>.
- 20 [44] Y. Chen, J. Shen, L. Huang, Y. Pan, X. Quan, Enhanced Cd(II) removal with  
21 simultaneous hydrogen production in biocathode microbial electrolysis cells in the  
22 presence of acetate or NaHCO<sub>3</sub>, *Inter. J. Hydrogen Energy* 41 (2016) 13368-13379,  
23 <https://doi.org/10.1016/j.ijhydene.2016.06.200>.
- 24 [45] B.E. Logan, Essential data and techniques for conducting microbial fuel cell and  
25 other types of bioelectrochemical system experiments, *ChemSusChem* 5 (2012)  
26 988-994, <https://doi.org/10.1002/cssc.201100604>.
- 27 [46] American Public Health Association, American Water Works Association, Water  
28 Pollution Control Federation, Standard methods for the examination of water and  
29 wastewater, 20th edn. American Public Health Association, Washington, 1998.
- 30 [47] Z. He, F. Mansfeld, Exploring the use of electrochemical impedance  
31 spectroscopy (EIS) in microbial fuel cell studies, *Energy Environ. Sci.* 2 (2009)  
32 215-219, <https://doi.org/10.1039/B814914C>.
- 33 [48] V. Madhavi, P. Jeevan Kumar, P. Kondaiah, O.M. Hussain, S. Uthanna, Effect of  
34 molybdenum doping on the electrochromic properties of tungsten oxide thin films  
35 by RF magnetron sputtering, *Ionics* 20 (2014) 1737-1745,  
36 <https://doi.org/10.1007/s11581-014-1073-8>.
- 37 [49] I. Andersson, J.J. Hastings, O.W. Howarth, L. Pettersson, Aqueous  
38 molybdotungstates, *J. Chem. Soc. Dalton Trans.* (1994) 1061-1066,  
39 <https://doi.org/10.1039/DT9940001061>.
- 40 [50] A. Katrib, V. Logie, N. Saurel, P. Wehrer, L. Hilaire, G. Maire, Surface electronic  
41 structure and isomerization reactions of alkanes on some transition metal oxides,  
42 *Surf. Sci.* 377 (1997) 754-758, [https://doi.org/S0039-6028\(96\)01488-4](https://doi.org/S0039-6028(96)01488-4).
- 43 [51] L. Huang, L. Gan, N. Wang, X. Quan, B.E. Logan, G. Chen, Mineralization of  
44 pentachlorophenol with enhanced degradation and power generation from air  
45  
46  
47  
48  
49  
50  
51  
52  
53  
54  
55  
56  
57  
58  
59  
60  
61

- cathode microbial fuel cells, *Biotechnol. Bioeng.* 109 (2012) 2211-2221, <https://doi.org/10.1002/bit.24489>.
- [52] L. Cao, W. Sun, Y. Zhang, S. Feng, J. Dong, Y. Zhang, B.E. Rittmann, Competition for electrons between reductive dechlorination and denitrification, *Front. Environ. Sci. Eng.* 11 (2017) 14, <https://doi.org/10.1007/s11783-017-0959-x>.
- [53] F. Jiang, Y. Zhang, N. Sun, Z. Liu, Effect of direct current density on microstructure of tungsten coating electroplated from  $\text{Na}_2\text{WO}_4\text{-WO}_3\text{-NaPO}_3$  system, *Appl. Surface Sci.* 317 (2014) 867-874, <https://doi.org/10.1016/j.apsusc.2014.09.031>.
- [54] W. Li, H. Yu, Z. He, Towards sustainable wastewater treatment by using microbial fuel cell-centered technologies, *Energy Environ. Sci.* 7 (2014) 911-924, <https://doi.org/10.1039/C3EE43106A>.
- [55] D. Jafarifar, M.R. Daryanavard, S. Sheibani, Ultra fast microwave-assisted leaching for recovery of platinum from spent catalyst, *Hydrometallurgy* 78 (2005) 166-171, <https://doi.org/10.1016/j.hydromet.2005.02.006>.
- [56] H.L. Le, J. Jeong, J.C. Lee, B.D. Pandey, J.M. Yoo, T.H. Huyunh, Hydrometallurgical process for copper recovery from waste printed circuit boards (PCBs), *Miner. Process. Extr. Metall. Rev.* 32 (2011) 90-104, <https://doi.org/10.1080/08827508.2010.530720>.

**Table 1** Separator factors in the 1# and the 2# units under various operational conditions

**Fig. 1** Effect of various W concentrations on rates of (A) W and (B) Mo deposition, (D) current, and (E) cathode potential in the stacked BESs. (C) Applied voltage and (F) hydrogen production in the 1# unit of the stacked BESs. (initial Mo(VI) fixed at 1.0 mM, initial pH: 2.0, cathode: SSS in the 1# and CR in the 2# units).

**Fig. 2** Effect of various Mo concentrations on rates of (A) W and (B) Mo deposition, (C) current, (D) cathode potential, (E) applied voltage, and (F) hydrogen production in the stacked BESs (initial W(VI) fixed at 1.0 mM, initial pH: 2.0, cathode: SSS in the 1# and CR in the 2# units).

**Fig. 3** XPS analysis for (A, C, E and G) W and (B, D, F and H) Mo elements on the cathodes of (A, B, E and F) the 1# and (C, D, G and H) the 2# units at W/Mo molar ratios of (A, B, C and D) 1 : 0.01 or (E, F, G and H) 0.01 : 1 (initial pH: 2.0, cathode: SSS in the 1# and CR in the 2# units).

**Fig. 4** EIS analysis at W/Mo molar ratios of (A) 1 : 1, 0.1 : 1, 0.05 : 1 and 0.01 : 1, and (B) 1 : 0.01, 1 : 0.05, 1 : 0.1 and 1 : 1 as well as (C) single W or Mo (initial pH: 2.0, cathode: SSS in the 1# and CR in the 2# units).

**Fig. 5** Effect of initial pHs on rates of (A) W and (B) Mo deposition, (C) current, (D) cathode potential, (E) applied voltage and (F) hydrogen production in the stacked BESs (W : Mo = 1 : 1; cathode: SSS in the 1# and CR in the 2# units).

**Fig. 6** XPS analysis for (A, C, E and G) W and (B, D, F and H) Mo elements on the cathodes of (A, B, C and D) the 1# and (E, F, G and H) the 2# units at an initial pH of (A, B, E and F) 1.5 or (C, D, G and H) 4.0 (W : Mo = 1 : 1, cathode: SSS in the 1# and CR in the 2# units).

**Fig. 7** Effect of cathode material on rates of (A) W and (B) Mo deposition, (C) current, (D) cathode potential and (E) applied voltage in the stacked BESs. (F) Rate of hydrogen production in the 1# unit of the stacked BESs (W : Mo = 1 : 1; initial pH: 2.0).

**Fig. 8** Rates of (A) W and (B) Mo deposition, (C) current, (D) cathode potential, (E) applied voltage and (F) hydrogen production as a function of equal W/Mo molar ratio (CR in the 1# unit and SSS in the 2 units, initial pH: 2.0).